Graduate Theses and Dissertations   Graduate School

2011

Thermal Response of Lithium Tantalate for Temperature Measurement

Ardit Agastra
University of South Florida, aagastra@mail.usf.edu

Thermal Response of Lithium Tantalate for Temperature Measurement

by

Ardit Agastra

A thesis submitted in partial fulfillment
of the requirements for the degree of
Master of Science in Mechanical Engineering
Department of Mechanical Engineering
College of Engineering
University of South Florida

Major Professor: Frank Pyrtle III, Ph.D.
Nathan Crane, Ph.D.
Craig Lusk, Ph.D.

Date of Approval:
March 24, 2011

Keywords: Pyroelectricity, Signal Amplification, Voltage Response, Modified
Wien Oscillator, Voltage Output

ACKNOWLEDGEMENTS

TABLE OF CONTENTS

LIST OF TABLES

LIST OF FIGURES

ABSTRACT

This thesis describes the study of the thermal response of the pyroelectric material named lithium tantalate or LT ($LiTaO_3$) in aid of this material's possible use for temperature measurement. The temperature range studied was between 5-99°C. The sensor was excited using a silicon rubber heater. The lithium tantalate sensor and the rubber heater were enclosed such that the temperature would reach steady state faster. The enclosure was a small insulated box in order to reduce any extraneous effects on the sensor. The output signal of the lithium tantalate sensor was then amplified by using four different amplifying circuits and the voltage output was studied. The amplifying circuits included Current Mode, double Current Mode, Voltage Mode, and a modified Wien Oscillator.

Results demonstrated linear dependencies of the voltage output as a function of temperature for the Voltage Mode and the modified Wien Oscillator. Using the modified Wien Oscillator amplifying circuit the slope of the line a 2.1mV/^{o}C and for the Voltage Mode the slope was 1mV/^{o}C. For both cases it was found that the range for the standard deviation of the measurements was 0.5<σ<1mV and the correlation coefficient R^2 was above 0.98. Results are comparable to theoretical results for the same amplifying circuits simulated with OrCAD Family Capture Lite Edition and PSpice 9.2 software.

The data showed that the lithium tantalate sensor could be used as a temperature measuring device for the range mentioned above. The resolution of the data is high enough to be able to be detected with modern measuring devices and the standard deviation is low enough to allow for such measurements. Moreover, the linear dependence of the data allows for accurate measurements at each temperature within the range.

CHAPTER 1: INTRODUCTION

Ferroelectricity and piezoelectricity are two material properties that are relatively new in science however they are more recognized than pyroelectricity. In terms of time since their discovery, piezoelectricity and ferroelectricity pale in comparison to pyroelectricity. The first two were discovered as a result of pyroelectricity about two millennia after pyroelectricity was first observed by Theophrastus, a philosopher of ancient Greece (Lang, 1999). He recognized that tourmaline, today recognized as a pyroelectric material, attracted other smaller objects when a change in temperature was present. Possible lack of understanding or apathy towards this subject made it difficult for this phenomenon to be recognized worldwide for almost two thousand years (Lang, 2004). Renaissance brought forth the interest in science and pyroelectricity was once again a part of research around the world. The new beginning of pyroelectric studies began in early 18th century and ever since it has become an important tool of modern science. This flowering in pyroelectric studies eventually leads to the naming of this phenomenon by David Brewster due to the fact that *pyro* means fire in Greek (Lang, 2005).

Particular solids fundamentally bear a spontaneous polarization whose intensity could be modified with a change in temperature, and this defines whether a material is pyroelectric. If a material, in the presence of a temperature gradient, has a net change in polarization then that is the definition of

1

pyroelectricity. In better terms, Lang (1974) defines the spontaneous polarization as the "non-zero polarization of a material in the absence of an external electric field." Thus, when there is a net charge created within a solid, an amassing of charges will appear on the surface as to cancel what is happening within the solid. This charge which accumulates on the surface could be measured using an ammeter after placing electrodes on the surface of the pyroelectric solid (Lang, 2005).

As mentioned above, temperature is essential in creating electricity in a pyroelectric material. Temperature itself is a quantity which has a recent history in terms of its measurement. It was not until the sixteenth century that temperature started being measured using an air thermometer developed by Galileo. Accurate temperature measurement is a recent development because one must first fully understand statistical mechanics or thermodynamics (Quinn, 1990). Since the first breakthrough from Galileo, temperature measurement has been flourishing with numerous different ways of achieving it. According to Quinn (1990) there are two types of thermometry: primary and secondary. In primary thermometry it said the temperature measurement is carried out without establishing any temperature dependent variables. An example of this type of thermometry is total radiation thermometry. On the other hand, secondary thermometry includes the rest of the methods used which do not fall under the previous category. Thermocouple temperature measurement is an example of secondary thermometry.

In the following paper many different thermometry methods and their applications are discussed. Also a review of pyroelectricity and its relevance will be communicated. The scope of this thesis entails the correlation between a pyroelectric measurement and the ambient temperature and the main purpose of it is to measure ambient temperature using a pyroelectric sensor. The chosen lithium tantalate sensor will be subjected to a temperature change and the output signal was analyzed and compared to the input temperature. The possible uses of such a correlation include but are not limited to medicine, military, imaging, electronics etc. The foundation of this thesis is based on developing a different method of temperature measurement using the pyroelectric material lithium tantalate which could be applied in any place where temperature measurement is necessary.

Lithium tantalate is a pyroelectric crystal which also exhibits ferroelectric properties. This sensor was enclosed such that the temperature would reach steady state and no extraneous effects would affect the sensor. The temperature was changed using a resistance heater and the sensor response was measured. The response measurement did require amplifying circuits to amplify the output signal. This circuit was implemented using a breadboard since changes to the circuit might be necessary. The amplified signal was then measured using an oscilloscope. The temperature of the enclosure was measured using thermocouples and was recorded for later use. Subsequently, the response of the sensor was compared to the temperature and correlations were sought between any characteristic of response against the temperature change.

CHAPTER 2: LITERATURE REVIEW

This literature review entails a look at temperature measurement, some methods of thermometry, and how they are used today. Moreover, an in-depth look is taken on pyroelectricty, its history and physics, and its importance in today's world. Also, a brief review of lithium tantalate is provided. In addition, new advancements in both fields are discussed. Both, temperature and pyroelectricity are in the center of this thesis as a different method to relate pyroelectricity to temperature is sought and possibly a new technique of temperature measurement could be developed.

2.1: Methods of Thermometry

As mentioned in the introduction, there are many different methods of temperature measurement. The past five centuries have seen a bloom in temperature measurement technology and thus there are numerous techniques by which one can measure temperature. In this section three different methods of thermometry are discussed: resistance thermometry, thermocouple, and radiation thermometry. These three methods were chosen because they are three of the most important and widely used methods today. The science behind each method is discussed and their importance is described.

2.1.1: Resistance Thermometry

Resistance thermometry relates a change in electrical resistance of a material to a change in temperature. According to Michalski et al. (2001), Sir Humphrey Davy was the first scientist to report in 1821 a correlation between the resistance of a material (platinum in this case) and a change in temperature. The beginning of resistance thermometry is accredited to a publication by H. L. Callendar in late 19th century on the dependence of electrical resistance of platinum on temperature. Despite some previous lack of success on a similar subject by Lord Kelvin and James Maxwell, H. L. Callendar pursued what he believed to be a new method of temperature measurement (Quinn, 1990). His success in this subject was a milestone in resistance thermometry as it became a subject of heavy research after his publication.

Although there are counter examples, most commonly the resistance of a material increases with an increase in temperature. This is attributed to the fact that an increase in temperature causes an increase in vibrations within an atom and thus the movement of free electrons is restricted (Michalski et al., 2001). With the assumption that temperature is the factor that affects the resistance of a material, then we can say that the equation for the resistance as a function of temperature is given by:

$$R_{\theta} = R_{\theta o} [1 + A\Delta\theta + B\Delta\theta^2 + C\Delta\theta^3]$$

Usually the coefficients A, B, and C are considered to be independent of temperature and their equations are given by:

$$A = 1/R_{\theta o} \ (\partial R_{\theta}/\partial\theta)_{\theta=\theta o}$$

$$B = 1/2R_{\theta o} \left(\partial^2 R_\theta / \partial \theta^2\right)_{\theta=\theta o}$$

$$C = 1/6R_{\theta o} \left(\partial^3 R_\theta / \partial \theta^3\right)_{\theta=\theta o}$$

In the above equations R_θ is the resistance and θ_o is the reference temperature which is often taken to be 0^oC. This is the case for the temperature sensing elements of a resistance thermometer called resistance thermometer detectors or RTDs. In addition to having a reference temperature of 0^oC, the equation for an RTD can be simplified further when the constant "C" is disregarded. With that said, there are a few factors to keep in mind when designing a resistance thermometer. According to McGee (1988), a few of these characteristics include but are not limited to:

1. high resistance per unit temperature
2. stable physical properties
3. adequate mechanical strength
4. possibly no hysteresis or path dependence

These characteristics are necessary in manufacturing an RTD whose uses range from simple every day measurements to very complex ones. The fore mentioned characteristics are also part of the material selection process which forms the basis for such designs.

When considering a wide range of temperature measurement, metals are the primary material choice for designing a resistance thermometer. These metals include but are not limited to: platinum, copper, and nickel. The table below shows each metal, its operating temperature, and the resistivity at 0^oC.

Table 1. Metals used for resistance thermometry and their properties (from Michalski et al. 2001).

Metal	Operating Temperature (^{o}C)		Resistivity
	Normal	**Special**	**($\mu\Omega$m)**
Nickel	-60 to 150	-60 to 180	0.09 to 0.11
Platinum	-200 to 850	-260 to 1000	0.10 to 0.11
Copper	-50 to 150	-50 to 150	0.017 to 0.018

Note: Reproduced from Michalski et al. 2010.

Although not mentioned on this table, another important figure of merit for such metals is the ratio of the resistance at 100°C to the resistance at 0°C called R_{100}/R_0. This figure of merit is really important in determining the purity of the material and thus gives a better understanding of the material's resistance (Quinn, 1990). In addition, another ratio "W" is used to compare materials. W is a resistance ratio and its equation is given by:

$$W=R/R_o$$

Where R is the resistance at any temperature and R_o is the initial resistance. This ratio of resistances provides a great way of comparison between materials with different initial resistances. The figure below shows what the resistance ratio, W would look like for an arbitrary material that is used for resistance thermometry (McGee, 1988).
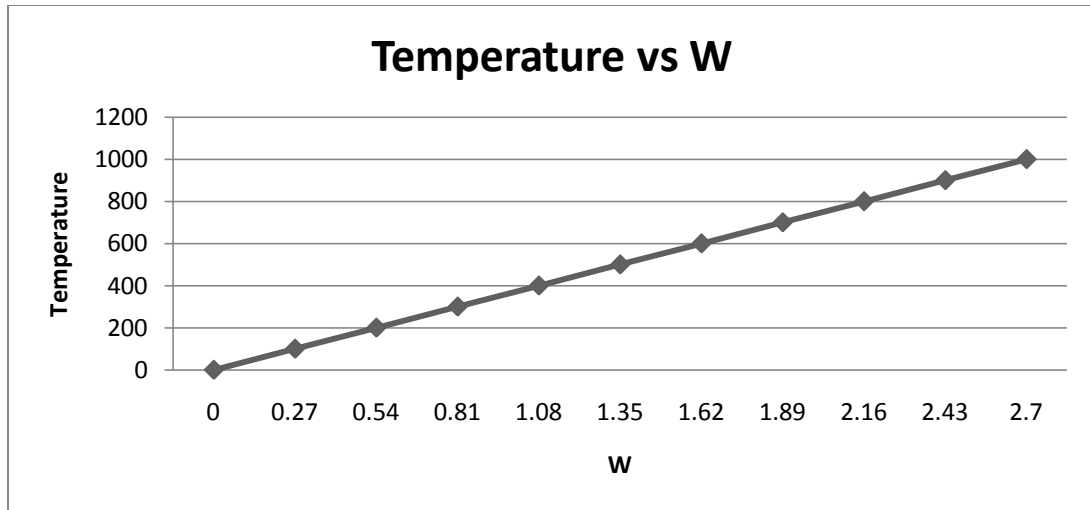
Figure 1. Graph for temperature vs. W for an arbitrary material that is used for resistance thermometry (from McGee, 1988).

In addition to metals, ceramics are widely used in resistance thermometry. A thermistor is considered to be a semiconductor with its resistance being many times more sensitive than that of metals. Some drawbacks that thermistors introduce are nonlinearity and decreased stability, but they are inexpensive and readily available for purchase. Moreover, they are used for applications where the precision of temperature measurement is at a minimum (Michalski et al., 2001).

Although thermistors are of importance in some applications, platinum resistance thermometers are the most reliable and widely used form of resistance thermometry. Platinum has been and is to this day the most frequently used material for resistance thermometers because of its wide range of use and the linearity between its resistance and temperature. It makes platinum resistance thermometers very practical in many resistance thermometry applications.

2.1.2: Thermocouples

Thermocouple temperature measurement is a method of thermometry that dates back to the findings of T. J. Seebeck in 1821. He discovered the effect which now takes his name in which he explains that two unalike metals create a current when their junctions are at two different temperatures (Quinn, 1990). According Michalski et al. (2001) two dissimilar thermal and electrical conductors joined at one end create a thermocouple. It is the end where the two conductors meet that the measuring point in created and the two open ends are considered reference points. Thermocouple temperature measurement only measures the temperature difference between the reference point and the measuring point and thus the reference temperature must be known. Usually a reference point is taken as the freezing point or the boiling point of water (0°C and 100°C respectively) with the former being the most preferred reference point. The temperature difference between the free ends and the junction point create a different voltage in each conductor. The introduction of a third electrical conductor is necessary to measure the voltage difference between the two dissimilar conductors (Kinzie, 1973). Depending on the conductors used, a table for the voltage between conductors against temperature is created. This would be used as a reference when using thermocouples. The tables are different for each set of conductors used. A simple thermocouple circuit is depicted in Figure 2. It shows two dissimilar materials X and Y and T_1 and T_2 could be arbitrarily the reference temperature and the temperature being measured.
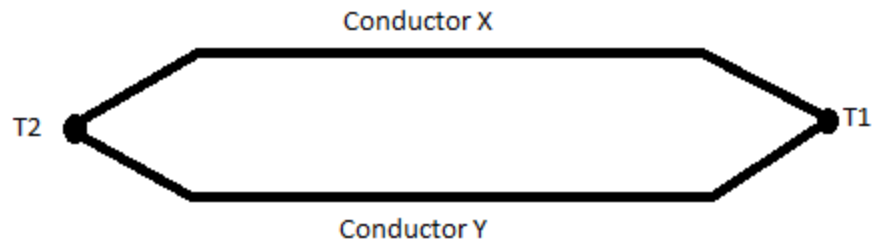
Figure 2. Simple thermocouple circuit (from Kinzie, 1973).

Materials selection is very important for thermocouple temperature measurement. Material choice determines the properties of the measuring system. It is necessary to optimize between the following properties of thermoelectric materials in order to get the best performing thermocouple:

1. high permissible working temperature

2. high resistance to oxidation

3. low resistivity

4. high melting temperature

5. possible linear relationship between electromotive force (Emf) and temperature

Moreover, it is extremely important to select two materials which create the highest Emf (electromotive force) or Seebeck voltage range. Table 2 shows some commonly used materials and the Emf values referred to platinum. This makes for the most appropriate thermocouples.

Table 2. The Emf values for different metals referred to platinum at 100°C with a reference temperature of 0°C (from Michalski et al., 2001).

Metal	Emf (mV)	Metal	Emf (mV)
Constantan (55%Ni-45%Cu)	-3.51	Iridium	0.65
Nickel	-1.48	Rhodium	0.70
Cobalt	-1.33	Silver	0.74
Palladium	-0.57	Copper	0.76
Platinum	0	Gold	0.78
Aluminum	0.42	Iron	1.98
Lead	0.44	Chromel	2.81

Note: Reproduced from Michalski et al. 2010.

The most common thermocouples used are type K and type E. Type K thermocouples are created by using one conductor made of nickel-chromium (Chromel) and the other made of nickel-aluminum. This is the most widely used thermocouple due to its range of use. Type E thermocouples on the other hand, use nickel-chromium (Chromel) and copper-nickel (Constantan) conductors respectively. This type of thermocouple is the preferred one in the United States since it has the highest range of Emf out of all metal thermocouple combinations (Michalski et al., 2001).

Kinzie (1973) explains in detail of a few applications of thermocouples. The author discusses thermocouple uses in fluid temperature measurement, manufacturing processes and heat appliance safety. Moreover, thermocouple temperature measurement is not limited to the applications mentioned above as it is used in many other smaller but nonetheless important applications.

Thermocouples are widely used due to the fact that they are low cost and reasonably reliable in many applications. One disadvantage that thermocouples introduce is lack of precision in certain temperature ranges. Overall,

thermocouples are easy to use and available to everyone. The extent of use of thermocouples is very important in many applications.

2.1.3: Radiation Thermometry

One may have heard of radiation pyrometry or infrared pyromtery and may have wondered if there is a difference between the two. These are two names which are used as synonyms for the method of thermometry by means of thermal radiation. Unlike the thermocouple or resistance temperature measurement, radiation thermometry could be explained explicitly through equations relating temperature to spectral radiance (Quinn, 1990). This method of thermometry is a noncontact method in which the device used does not touch the material whose temperature is being measured. Moreover, because the equations for this method could be written explicitly, it falls under primary thermometry.

The fundamentals of radiation thermometry come from the Stefan-Boltzmann law of thermal radiation. According to this law, the energy flux leaving a surface (W/m^2) is proportional to the fourth power of that body's temperature. The most important aspect of thermal radiation is the emissivity of the target (Zhang et al., 2010). To understand the process of thermal radiation and how emissivity plays a role one must first study blackbody radiation. A blackbody is used as a comparison device when discussing radiation. It is a perfect surface in which three important steps happen:

1. it absorbs all incident radiation
2. no other surface can emit more radiation

3. all radiation is emitted isotropically (same intensity in all

directions)

These are the three reasons why a blackbody is called the "ideal radiator" and all

real surfaces are compared to it (DeWitt et al., 1988). With that established we

can say that emissivity has a range between 0 and 1 with a blackbody having an

emissivity value of 1. But getting the exact emissivity of a surface is an arduous

task. Over the years techniques to overcome this problem have been created.

Some techniques to reduce emissivity problems include dual-wavelength

pyrometers, multi-spectral thermometry and reflective mirrors (McGee. 1988).

According to Zhang et al. (2010), the equation relating temperature,

emissivity and the total radiation excluding reflection is given by:

$$L_{em}=\varepsilon\sigma T^4/\pi$$

where L_{em} the total radiation emitted, ε is the emissivity of the body, T is the

temperature of the body, and σ is the Stefan-Boltzmann constant. Because a real

surface radiation is being measured, the directional emissivity and the total

radiance temperature never surpass and at most would equal that of a blackbody

(Zhang et al. 2010).

One of the earliest and probably the simplest methods of radiation

thermometry was the use of vision to detect the color emitted by the body in

question. With a well-trained eye, one can estimate the temperature of a body

within a few degrees and it is said that the human eye could distinguish a color

difference that corresponds to a $1^{o}C$ change in temperature. This could be useful

for heat treatment processes (Plumb, 1972). Table 3 demonstrates the

correlation between thermal radiation color and the temperature of the body.

Table 3. Temperature (800-1320°C) and radiation color correlation (from Michalski et al., 2001).

Temperature (^{o}C)	Color
800-830	Orange/carmine
830-880	Dark orange
880-1050	Orange
1050-1150	Yellow/orange
1150-1250	Yellow
1250-1320	White/yellow

Note: Reproduced from Michalski et al. 2010.

Since the first days of thermal radiation many attempts have been made

towards improving the main problems of thermal radiation. According to Zhang et

al.(2010) some of the more relevant problems are:

1. establish the target emissivity

2. surface conditions

3. angle of view

4. reducing contiguous radiation and other effects

The methods of improvement are solved by using two types of pyrometers.

Manually operated pyrometers are one method of pyrometry and include filament

disappearing and two-color pyrometers (Michalski et al., 2001). In filament

disappearing pyrometry the brightness of a lamp filament is changed by adjusting

the current input. The current is adjusted until the filament color becomes one

with the background color and the current then is compared to the temperature.

In two-color pyrometry, the ratio of the radiance emitted at two different

wavelengths is measured and thus inducing a temperature measurement. These

two methods solve the problems the surface conditions might create (Plumb,

1972). The rest of the problems are answered by automatic pyrometers which

are divided into two categories: optical and thermal or total radiation. The automatic optical pyrometers take advantage of the light emitted by the body and the thermal radiation pyrometers use the whole thermal radiation range to measure temperature (Quinn, 1990).

Moreover, photoelectric pyrometers use materials such as Germanium and Silicon to measure temperature. They are limited by the range of wavelength they could operate in. The table below shows these two materials and some of their properties.

Table 4. Some properties for germanium and silicon (from Michalski et al. 2010).

Wavelength, λ				
Material	Maximum Sensitivity (μm)	Maximum Operating Value (μm)	Resistance (Ω)	Time Constant (μs)
Germanium	1.2	1.8	--	1
Silicon	0.9	1.2	10^7	~1

Note: Reproduced from Michalski et al. 2010.

Some of the most important materials used in radiation thermometry are ferroelectric and pyroelectric materials. Pyroelectric materials intrinsically carry optical and thermal properties which could be related to temperature. Thus, a pyroelectric sensor was chosen and thermal radiation was used to perform the studies is search of a new way of measuring temperature.

2.2: Applications of Thermometers

Thermometry is useful in any application in which temperature measurement is necessary. The possibilities for temperature measurement are virtually endless. New research is being conducted on a daily basis in search of different methods of temperature measurement. Innovative temperature measurement techniques have been created in recent years which have many

different applications. According to Zhang et al. (2010) some of these techniques include but are not limited to:

1. ultrasonic thermometry (uses changes in the speed of sound to measure temperature

2. microwave radiometry (uses energy in the microwave range to measure temperature)

3. spectroscopic thermometry (uses visible light to measure temperature)

4. acoustic thermometry (uses changes in the speed of sound to measure temperature)

Some of these methods are currently in use and others are yet to be put on the market for commercial use. Nonetheless, applications for such systems have been defined.

For temperature measurement techniques such as the one mentioned in the previous section, applications are numerous. According to Zhang et al. (2010), radiation thermometry is widely used in metal processing industries such as steel and aluminum production. Moreover, the authors go in detail for a few more uses of radiation thermometry. Some of these uses include:

1. medical thermometry

2. sensing of earth surface temperature

3. thermal imaging in firefighting

4. military night vision

These are just a few applications where thermometry is exceptionally important. Scientists will continue to develop new methods for new application and the field of thermometry will keep growing. More accurate temperature measurement techniques will be sought after. Demands for such techniques will continue to increase as temperature measurement is important in numerous applications.

2.3: Pyroelectricity: Its History and Physics

The first writings on pyroelectricity date back to the days of the ancient Greeks when Theophrastus noticed that tourmaline attracted other materials in the presence of a fire (Lang, 1981). The next studies on this occurrence were not performed until the beginning of the renaissance. A few centuries later David Brewster coined the name "Pyroelectricity" to this phenomenon due to the fact that *pyro* means fire in Greek (Lang , 1974). The studies on pyroelectricity of the past century have brought to light some very important applications. Some other phenomena such as ferroelectricity and thermoelectricity were discovered by scientists whose previous works included pyroelectricity. The difference between ferroelectricity and pyroelectricity will be explained in a later section. In the early 1900s scientists discovered that pyroelectric materials could be used for infrared imaging. This was a step that would escalate the number of pyroelectric studies performed. It has led to numerous applications which range from medical imaging to space missions and beyond (Lang, 2005).

Like many other phenomena, everything in pyroelectricity begins at the atomic level. It is known today that the distance between positive and negative

charges is called the electric dipole moment. The total measure of the electric

dipole moments for a system is referred to as its polarity (Yan et al., 2007).

Change in temperature either increases or decreases the energy in a

system of atoms and therefore alters the crystal structure within. In the presence

of a temperature change a material's polarity is affected (Lovinger, 1983).

Supposing that we can get a crystal to be cut in such a way that the negative and

positive charges of the system are oriented towards the largest face in area of

the crystal, we can then attach electrodes on this area in order to measure the

electrical potential (Smith & Amon, 2007). This electrical potential can only be

measured if a pyroelectric material is subjected to a change in temperature. Lang

(2005) gives a more detailed look at how one could measure the pyroelectric

current generated by a material. It is also necessary to point out that the

polarization created by these materials is spontaneous and dies off after a critical

temperature is reached (Lang, 1974). Pyroelectricity, therefore, should not be

mistaken for thermoelectricity in which a fixed temperature profile allows a stable

electrical potential. In thermoelectricity, a change in temperature causes

electrons or electron holes to travel from one side to the other thus generating an

electrical current (Kinzie, 1973). In pyroelectricity, a change in temperature

causes electrons from the ambient to be attracted to the surface of the material

due to changes occurring within the material (Lang, 2005). Thus, in

thermoelectricity the electrical potential is generated by the electrons which

reside inside the volume as compared to pyroelectricity where electrons are

accumulated on the surface.

A simple representation of the equivalent circuit for a pyroelectric material or detector is given in Figure 3.
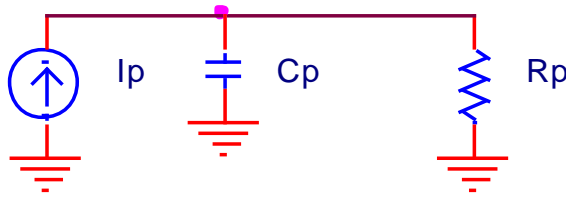
Figure 3. Equivalent circuit for a pyroelectric material (from Nalwa, 1995).

In the figure above the pyroelectric current is given by I_p, its resistance R_p and its capacitance C_p. The pyroelectric current is usually in the range of pico amperes and its resistance is in the order of 10^{12} ohms or higher. The capacitance varies with temperature and is in the order of pico farads (Kohli, 1998).

The current flowing in a circuit due to the presence of the pyroelectric material can be presented by the following equation

$$i_p = Ap(dT/dt)$$

where A is the area of the electrodes placed on the material, p is the pyroelectric coefficient acting perpendicular to the electrodes and dT/dt is the change of temperature with respect to time (Dietze et al., 2008). Most pyroelectric materials generate currents in the range of pico amperes and can reach micro amperes in some cases. Although these currents are relatively low, they are high enough to be used in numerous applications. Often other circuit components are used in parallel or in series with the material in order to improve the output signal of a device (Shaldin et al., 2007).

In order to improve the performance of pyroelectric materials a method called poling is often used. In poling one can change the dipoles in such a way

19

that they are oriented in the same direction and thus increasing the possible current generated by the material. According to Batra et al. (2008) there are six types of poling: plasma, hysteresis, electrical, thermal, corona, and electronic beam poling. All six of these poling procedures are used in poling of composites but electrical poling is widely used in crystals and other material groups. In electrical poling, a high electrical current is passed through the material to reorient the dipole moments within the material. Safari et al. (1996) demonstrated poling effects on a material. For a material that has not been poled, the dipoles within the crystal structure point in random directions, whereas in a poled material the dipoles are oriented to complement the electrical field applied during poling. Poling is a process which can improve the current output of the pyroelectric material as well as improve the responsivity of the device (Li et al.,2008).

It is beneficial to mention that ferroelectric materials are very similar to pyroelectric materials. As a matter of fact all ferroelectric materials are pyroelectric materials but not all pyroelectric materials are ferroelectric. This is the case because all ferroelectric materials have spontaneous polarization which can be reversed in the presence of an electric field. On the other hand, there are some pyroelectric materials that do not possess this quality therefore they are not ferroelectrics (Fedosov & Von Seggern, 2008).

2.4: Pyroelectric Materials

Pyroelectric materials are often known for their piezoelectric and ferroelectric properties. Three big groups can summarize the pyroelectric

materials which include crystals, polymers, and ceramics although minerals and biological materials are some other groups which have been considered (Fukada, 1989). All these groups have their own advantages and their specific uses. This section will give an overview of each group, describe some materials and their uses, and give some advantages for each material.

2.4.1: Pyroelectric Detectors

Pyroelectric detectors use pyroelectric materials to measure changes in temperature by measuring changes in heat radiation. The heat radiation is detected by the pyroelectric material which in turn sends a signal to the rest of the components. The information is then filtered by the other circuit elements, giving off a reading for the temperature change. Determining the electrical response is not an easy task. Analysis of these electrical and thermal components is required in addition to calculating the losses (Lau et al., 2008). While this proves to be a tough task, pyroelectric applications are too beneficial not to create pyroelectric detectors.

2.4.2: Pyroelectric Crystals

Crystals in general are divided into thirty two groups in which 20 groups show piezoelectric properties. Out of those 20 groups, 10 show spontaneous polarization and these are the pyroelectric crystal groups. A better understanding of the crystallographic groups is given in Table 5. Some pyroelectric crystals include Lithium Tantalate, triglycine sulfate, and strontium barium niobate. Crystals are beneficial because they give a high voltage response and most of

the crystals have high Curie temperatures which give a higher range of use

(Shaw et al., 2007).

Table 5. Pyroelectric and piezoelectric point groups (from Safari et al. 1996).

Crystal Structure	Non-centrosymmetric	
	Piezoelectric	Pyroelectric
Triclinic	1	1
Monoclinic	2, m	2, m
Orthorhombic	222,	mm2
Tetragonal	4, 422, 4mm, 42m	4, 4mm
Trigonal	3, 32, 3m	3, 3m
Hexagonal	6, 622, 6mm, 6m2	6, 6mm
Cubic	23, 43m	

Note: Reproduced from Safari et al. 1996.

2.4.3: Pyroelectric Polymers

The most recognizable polymer used in pyroelectric applications is

polyvinylidene fluoride (PVDF). This polymer is widely used in medical

applications due to the fact that its density is about that of human tissue and

water. In addition, polymers are very flexible and can be of use in many other

applications (Safari et al., 1996). Another advantage of polymers such as PVDF

is that they are commercially available in large-area thin films. Polymers are good

contenders for applications such as intruder alarms and single element devices

(Whatmore, 1986).

2.4.4: Pyroelectric Ceramics

Lead zirconate titanate is a very useful ferroelectric oxide and is one of the

most studied pyroelectric materials. PZT is a ceramic and offers different benefits

over other materials. It has advantages over crystals in the sense that it is easy and fairly inexpensive to manufacture and is chemically and mechanically strong (Batra et al., 2006). Moreover, ceramics allow for use in higher temperature ranges due to their high Curie temperatures.

2.5: Pyroelectric Properties and Figures of Merit

Material properties characterize an engineering material. They are what engineers and scientists first look at when making a material selection. The blueprint of a material is withheld within its properties and each material has its own distinct blueprint. Diamond is known for its hardness for example and copper is known for its corrosion resistance and these properties decide when and where such material will be used. Similarly, pyroelectric materials have their own properties that describe everything about the material. An understanding of the material properties is fundamental in any engineering discipline. This section of the paper explains some of the most important properties of pyroelectric materials and devices and why they are important.

2.5.1: Pyroelectric Coefficient

The pyroelectric coefficient is the relation between the change in temperature and the change in polarization of a material. The pyroelectric coefficient has units of C/Kcm^2. According to Wong (1993), there are two types of pyroelectric coefficient: one experimentally measured and the other one defined thermodynamically. They are given in the following forms

$$p_y(experimental) = 1/A \ (dQ/dT)$$

$$p_y(thermo) = dP/dT$$

where dQ/dT and dP/dT represent the change in charge and the change in polarization with respect to temperature respectively (Uchino, 2000). The experimental pyroelectric coefficient is usually lower in value than the thermodynamic one.

There is a distinction which should be made between two types of electrical responses in a pyroelectric material. Primary pyroelectricity is due to the change in temperature when keeping a constant volume for the material. But when temperature changes so does the volume which creates a secondary pyroelectricity due to the piezoelectric effect (Zheng et al., 2008).

Table 6. Some pyroelectric materials and their primary and secondary pyroelectric coefficients (from Lang 2005).

Material	Primary ($\mu C/m^2K$)	Secondary ($\mu C/m^2K$)
$BaTiO_3$	-260	60
$LiNbO_3$	-95.8	12.8
$LiTaO_3$	-175	-1
Tourmaline	-0.48	3.52

Note: Reproduced from Lang 2005.

The pyroelectric coefficient is the single most important property when choosing a pyroelectric material.

2.5.2: Responsivity

Responsivity is a measure of how well a detector is performing. The responsivity of a device is a measure of the ratio of the total voltage output compared to the total power input. This feature of a pyroelectric detector tends to decrease when heat radiation frequencies reach above 200 Hz. The higher this attribute, the better the detector works (Chvatal et al., 2009). This characteristic

24

for infrared detectors was studied in more detail by Batra et al.(2008). This property of pyroelectric detectors shows a great deal about the detectors themselves as well as their performance capabilities.

Whatmore (1986) studies pyroelectric devices in detail. He explains that for a pyroelectric detector the voltage response R_v is one of the more important aspects and is given theoretically by

$$R_v = (RpA\omega\eta)/[G(1+\omega^2\tau_t^2)^{1/2}(1+\omega^2\tau_e^2)^{1/2}]$$

where

G	is the thermal conductance
R	is the pyroelectric resistance
p	is the pyroelectric coefficient
τ_t	is the thermal time constant
τ_e	is the electrical time constant
η	is the emissivity
A	is the active area
ω	is the frequency

Moreover, the theoretical voltage response maximizes when the $\omega=(\tau_e\tau_t)^{-1/2}$. It should be noted that detectors are manufactured for specific tasks, thus this is a general property of a detector. Other properties might be more useful when developing a pyroelectric detector.

2.5.3: Noise

Noise becomes a problem when trying to get a small signal output from a device. For pyroelectric devices, Whatmore (1986) explained that there are four

dominant sources of noise to consider. They are temperature noise (noise generated by temperature when the system is in equilibrium, Johnson noise (noise created by the pyroelectric conductance), amplifier noise (noise generated by amplifying circuit), and finally current noise. The equivalent noise for a detector is given by Batra et al. (2008) as

$$\Delta V_N{}^2 = \Delta V_T{}^2 + \Delta V_J{}^2 + \Delta V_i{}^2 + \Delta V_A{}^2$$

Furthermore, a graph showing each noise as a function of frequency was proposed by Whatmore (1986) and is shown in the figure below.
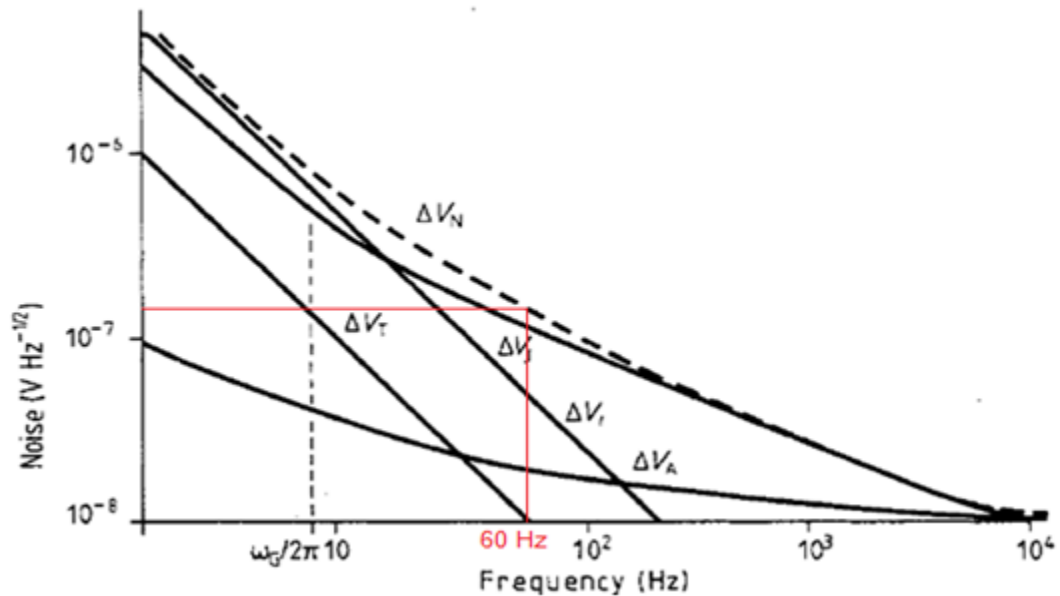
Note: Reproduced from Whatmore (1986).
Figure 4. Magnitudes of voltage noise for a pyroelectric detector as a function of frequency (Whatmore, 1986).

It is safe to say that from the graph, that the Johnson noise dominates after 20 Hz and before that the current noise dominates. All the noises should be at their lowest for a good performing detector. It is important to note that for this thesis, the frequency used in 60 Hz. At this frequency the voltage noise is approximately

26

four orders of magnitude smaller (~10^{-7} V) than the signal that is being measured (10^{-3}V). It is assumed that the noise has negligible effects on the output signal.

2.5.4: Curie Temperature

The Curie temperature would be thought of as a limitation of the pyroelectric material in the sense that the spontaneous polarization of the material dramatically decreases as the temperature is increased to the Curie temperature. It is the temperature at which the material's polarization goes to zero (Ramos et al., 2007). Careful attention should be paid to the Curie temperature of a material because it could be the limiting factor for the application in which the pyroelectric material is being used. Detectors in general use different types of materials due to the different properties and figures of merit materials exhibit (Kao, 2004).

Table 7 shows some pyroelectric materials and their respective figures of merit. These are some of the widely used pyroelectric materials. These properties include the pyroelectric coefficient, loss tangent (a way to quantify the energy dissipation within a material), strain, and Curie temperature. Specific applications of such materials require careful attention to certain figures of merit.

Table 7. Pyroelectric materials and their figures of merit (from Xiao et al. 1988).

Material	p (10^4C/m^{2}K)	tanδ	ε	T_c (^{o}C)
PVF$_2$	0.27	0.015	12	170
TGS	5.5	0.025	55	49
PZT	3.8	0.003	290	230

Note: Reproduced from Xiao et al. 1988.

2.6: Pyroelectric Current State of Research

Recent years have seen pyroelectric research advance to new levels. This section takes a look at recent papers and an overview of their areas of research.

Mischenko et al. (2008) looks into harvesting waste energy and turning it into electrical energy using the pyroelectric phenomenon. The authors propose the idea of using a pyroelectric material in places where heat is lost such as air conditioning to convert that heat into electricity. At this point efficiencies for this conversion are very low but there is room for improvement. This is a very young area of study but there is a lot to be discovered.

Continuing on those steps, Vanderpool et al. (2008) take a look at conversion of waste heat directly into electricity. In this paper, a prototypical energy converter is simulated and studied by solving two dimensional energy, mass, and momentum equation using the finite element method. Results demonstrate that there is an energy efficiency increase with an increase in specific heat and density of the working fluid and the pyroelectric material. They calculated a possible efficiency of 40% for Carnot Cycle.

Moreover, Guyomar et al. (2009) take a look at the harvesting of thermal energy using a pyroelectric material. A method called synchronized switch harvesting on inductor (SSHI) is used to perform experiments. For the Carnot cycle the efficiency of energy harvesting is about 0.05%. In this case the power produced for a temperature change of 7K is more than 0.3 mW for an active material that has a mass of 8g. Temperature frequency seems to be the limiting

factor is this case. Large temperature variations are necessary to increase the efficiency and low speed of heat transfer makes it difficult to achieve that.

Qiu-lin et al. (2009) take a look at gas sensors as an important application of pyroelectric materials. These sensors can be used to measure the amount of gas in the environmental level, in biomedical devices, and automobiles. In this article, thin film pyroelectric materials are studied for this particular use. The pyroelectric sensor detects infrared waves of the gas produced then coverts it into an electrical signal. This paper studies the detection of methane gas and the results show that these pyroelectric sensors are good candidates for such tasks.

Epstein et al. (2009) introduce the electrocaloric effect (ECE) which is a phenomenon similar to pyroelectricity. When an electric field is applied to an electrocaloric material the temperature rises and when the field is decreasing, the temperature goes down. In this paper, the properties of electrocaloric materials are studied for application such as refrigeration, heat pumps, and electrical generators. The efficiency of refrigerators and generators using thin-film electrocaloric materials are studied. It is shown that the efficiency increases with an increase of the thermal conductivity between the heat switches. These refrigerators and generators are comparable to today's thermoelectric devices.

Lead zirconate titanate and polyvinylidene fluoride are two materials that are studied in paper by Cuadras et al. (2010). The authors propose these two materials as thermal energy harvesting sources to supply a low-power autonomous sensor. The sensors are used as current sources with output impedances. Heating and cooling of the sensor is created by air currents. The

29

generated currents were in the order of 10^{-7} Amperes. This current is collected in a capacitor for cooling and heating cycles. The energy collected was measured up to 0.5 mJ, which is enough to power a sensor making measurements such as mentioned above.

Recent studies concerning pyroelectric materials concentrate more on applications of pyroelectric materials in such areas as infrared detection, gas monitoring and energy harvesting. Not many studies concentrate on the effects of temperature on such materials. This thesis will require the use of a pyroelectric sensor and study the temperature dependence of its properties in hope of developing a new method for temperature measurement.

2.7. Lithium Tantalate

All ferroelectric materials are considered to be pyroelectric but not vice versa. This means that the direction of the dipole moments could be reversed in the presence of an electric field but the rest of the properties of ferroelectric materials follow pyroelectric behavior. As was mentioned above, lithium tantalate or usually known as LT is a ferroelectric crystal. LT has a Curie temperature of ~610°C and is one of the most widely used pyroelectric/ferroelectric materials. Lithium Tantalate is used in many different applications such as human detection, military, and security (Nougaret et al., 2009) and lately it has received a lot of attention for electro-optical applications (Satapathy et al., 2011). Lithium tantalate is widely used in such applications due to the following properties:

1. high mechanical stability (Sokoll et al., 1997)

2. low thermal expansion (Sokoll et al., 1997)

30

3. high signal-noise-ratio (Norkus et al., 2010)

4. reproducibility of sensor properties (Norkus et al., 2010)

Some fabrication methods for lithium tantalate include ion beam etching, sol-gel method, and radio-frequency magnetron sputtering (RFMS). In ion beam etching a similar process to sand blasting is created where single atoms to ablate the material away (Sokoll et al., 1997). In the sol-gel method or chemical solution deposition as it may be called, a solution is used to create a gel-like structure and then the material itself (Satapathy et al., 2011). Other methods include deposition by RFMS, thermal evaporation, and laser ablation (Nougaret et al., 2009). LT can be fabricated to fit many applications and is readily available.

Most of the recent studies involving lithium tantalate are concerned with this material's optical properties. Although pyroelectric properties and applications of this material have been studied, studies today concentrate of electro-optic applications. Kohli et al. (1998) has studied the electrical and pyroelectric properties of LT. Most of the experimental results on this study are concerned with how a property varies with a change in frequency. They studied the relative permittivity (how well energy is stored within the material) of a capacitor created from this material and its variance with temperature for the range 110-610°C. Results showed a linear dependence of the relative permittivity for ranges 110-310°C and 350-550°C. Nothing has been mentioned on how this could be used for possible temperature measurement. Moreover, these results are out of the scope of this thesis as the range of temperature studied in this thesis is 0-100°C. Furthermore, Jacob et al. (2004) studied the permittivity and

loss tangent of lithium tantalate as a function of temperature. Tests were performed for a frequency 11.44 GHz and for temperatures up to 300K. Again, this temperature range is out of the scope of this thesis. Moreover, lack of state-of-the-art testing equipment would not allow for such measurements at the temperature range of 0-100°C.

This thesis is based solely on the thermal response of this material and it could be looked at as a starting point for temperature measurement using lithium tantalate. In this thesis, any extraneous effects on the lithium tantalate sensor were eliminated and the response will be purely dependent on the temperature change. Moreover, all types of noise were minimized by the manufacturer of the sensor. The main purpose was to study only the temperature effects on the sensor while other effects were eliminated or at the least are kept at a minimum.

CHAPTER 3: MATERIALS AND METHODS

In this chapter the materials, instrumentation, and the methods that were necessary to complete this thesis are discussed. A detailed look at the materials and instrumentations used are provided. Moreover, a step by step presentation of the experimental setup is given. This chapter is presented in such a way that someone could easily reproduce this experiment.

3.1: Materials and Instrumentation

After careful research of pyroelectricity and pyroelectric materials it was decided that the best material to use for this project was lithium tantalate ($LiTaO_3$). A few important factors were considered when making the selection. One factor was that secondary pyroelectricity of $LiTaO_3$ is almost zero and is the lowest among the most commonly used materials as shown in Table 6. This allows one to study in higher accuracy the temperature dependent properties of this material/sensor as the volumetric effects will be neglected. Moreover, lithium tantalate has a high Curie temperature ($\sim 610^{o}C$) which allows for higher temperature studies (although not necessary for this thesis due to its scope). Another advantage of such a sensor is its high current response. This means that the current or voltage output of the sensor compared to the power input is relatively high when compared to other sensors. The sensor was ordered from a manufacturer located in Oregon and the company name is Spectrum Detector. According to their manual some additional advantages of such a sensor are:

1. fast response time

2. small and portable

3. used in current mode and voltage mode circuits

4. highly sensitive

This sensor is named SPC-2 meaning it is a discrete pyroelectric detector with a diameter of 2mm. According to the manufacturer, this sensor has a broadband of 0.1 to 100μm. Moreover, it is specifically manufactured to be used as an optical pyrometer, laser energy meter, and infrared gas sensor. The purpose of this thesis is to show that this sensor could be used something other than what is specified by the manufacturer: a starting point for possible temperature measurement. Furthermore, some of the specifications for this sensor according to the manufacturer are shown in Table 8 below and Figure 4 shows a close-up photograph of the sensor.

Table 8. Specifications for SPC-2 LiTaO$_3$ pyroelectric detector.

Parameter	Magnitude
Diameter (mm)	2
Area (mm^2)	3.14
Capacitance (pF)	22
Thermal 3db Frequency (Hz)	1.6
Current Responsivity (μA/W)	0.45
Maximum Average Power (mW)	50

Note: Reproduced from manufacturer's manual.

Figure 5. SPC-2 Lithium Tantalate pyroelectric sensor.

In order to measure the temperature response of the Lithium Tantalate sensor mentioned above I must have the sensor enclosed in such a way that any convective and optical effects on the sensor would be neglected. I chose a well insulated box with dimensions of 5"x4"x1". Polyurethane was used to insulate the walls of the enclosure. This was used due to the fact that it has a high enough temperature limit (~120°C) to be used for this thesis. Two sheets of polyurethane with dimension 5"x4"x¼" were used to insulate the top and the bottom of the box, two rectangles of dimension 5"x ½"x¼" were used to insulate the sides along its length and two more with dimensions 3"x ½"x¼" were used to insulate along its width. The reason for choosing such a small box is to make sure that steady state temperature would be achieved faster.

A type-k thermocouple was chosen for temperature measurement of the ambient inside the enclosure. The accuracy of the thermocouple was 0.4% of the temperature being measured. For the measurements made in this thesis the highest uncertainty would be at 99°C (0.004*99°C=0.396^{o}C). The temperature was read from an Omega HH12A digital thermometer. The uncertainty of the

35

digital thermometer is half of its resolution ($0.5*1^{o}C=0.5^{o}C$). The digital

thermometer thus is the limiting instrument for the measurements made in this

thesis.

A silicon rubber heater was used to increase the temperature within the

enclosure. This heater was purchased from Omega.com. Moreover, a mini fridge

was used to decrease the temperature of the sensor below the room

temperature.

In order to amplify the signal output, four different amplifying circuits were

used. The first two are called Voltage Mode and Current Mode and are proposed

by Chirtoc et al. (2003). Representations of these two amplifying circuits using

OrCAD 9.2 Capture CIS Lite Edition are given in Figures 5 and 6.
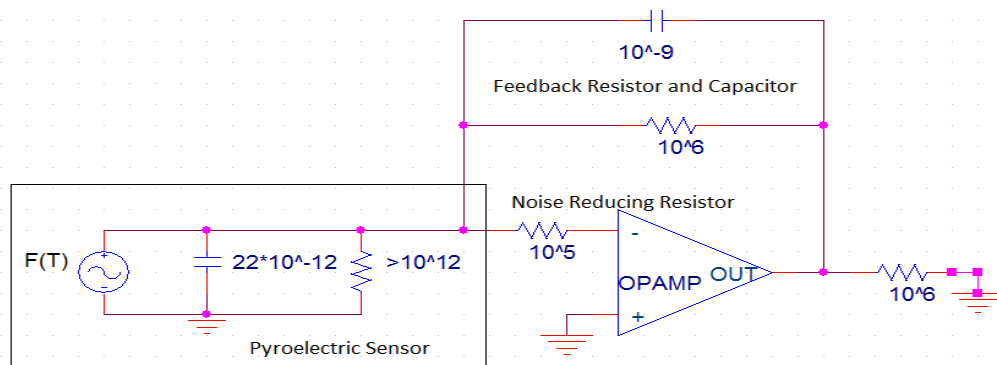
Note: Reproduced from Chirtoc et al. (2003).

Figure 6. Current Mode amplification circuit as proposed by Chirtoc et al. (2003).
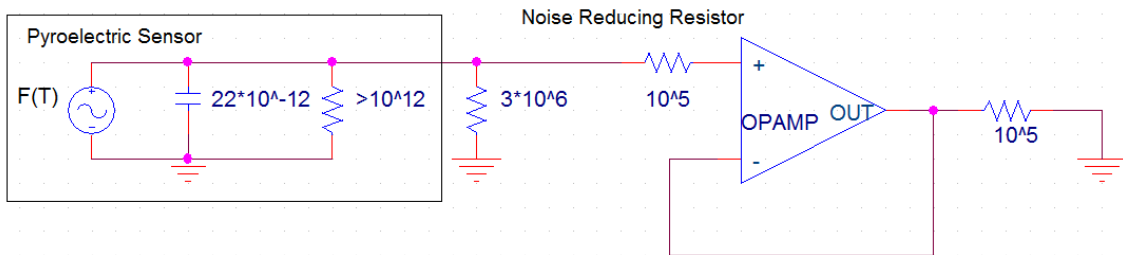
Note: Reproduced from Chirtoc et al. (2003)

Figure 7. Voltage Mode amplification circuit as proposed by Chirtoc et al. (2003).

Moreover, a double Current Mode amplifying circuit was used as proposed by Chung et al. (1996). An illustration of this circuit using OrCAD 9.2 Capture CIS Lite Edition is given in Figure 7.
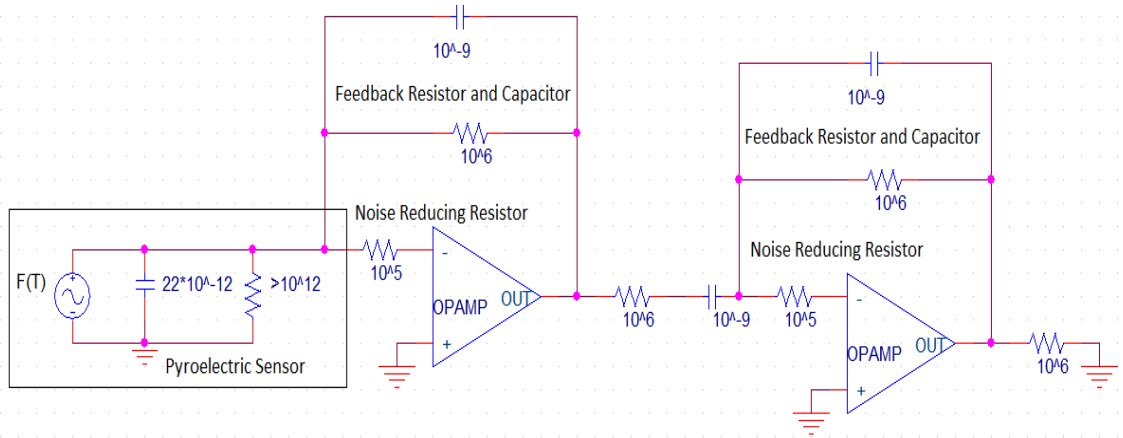
Note: Reproduced from Chung et al. (1996).
Figure 8. Amplification circuit as proposed by Chung et al. (1996).

And last but not least I used an amplification circuit using a modified Wien Oscillator as proposed by Malhame (2002). A demonstration of this circuit using OrCAD Capture CIS Lite Edition 9.2 is given in Figure 7. The difference between this amplifying circuit and the Wien Oscillator is that the pyroelectric sensor is replacing a capacitor and resistor in series.

37

10^6

10^6
Noise Reducing Resistor

R7   OPAMP OUT

10^5

100*10^-12   10^6

F(T)

>10^12   22*10^-12   10^6
Shunt Resistor

Pyroelectric Sensor

10^5
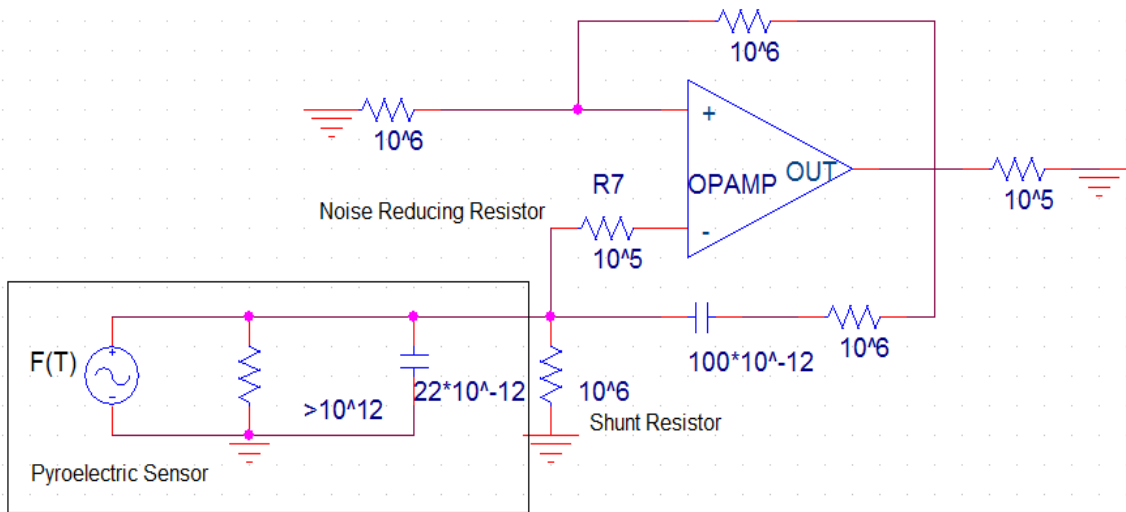
Note: Reproduced from Malhame (2002).

Figure 9. Modified amplification circuit similar to a Wien Oscillator circuit proposed by Malhame (2002).

The components used to build these amplifying circuits were purchased from

RadioShack. A summary of these components is given in Table 9.

Table 9. Components used for the amplification circuits.

Component	Type	Value	Amount
Resistor	½ watt 5%	$10^6 \ \Omega$	11
		$10^5 \ \Omega$	7
Capacitor	ceramic-plate	10^{-9} F	4
		10^{-10} F	1
Operational Amplifier	741 OP AMP mini DIP IC	NA	5
Electrical Breadboard	No. 276-001	5V max	2

A few additional instruments were necessary for measurement of the

signal. A DC power supply was used to supply power to the breadboard and its

components. Moreover, another AC power supply (60Hz) was used to supply

power to the silicon rubber heater. The power output of the AC power supply was

monitored using a digital voltmeter. An oscilloscope purchased from Agilent

Technologies was used to measure the signal output. And last but not least a

personal computer was used to document the data and produce the necessary graphs. The data was recorded into Microsoft Office Excel 2007 and the graphs were generated.

3.2: Experimental Setup

Before beginning the experiment, the amplifying circuits needed to be constructed using the components purchased from RadioShack (resistors, capacitors, operational amplifiers, and electrical breadboards). Careful attention was paid to the design of the circuits when using of the breadboard and the operational amplifiers. A small misplacement of the components on the breadboard result in the wrong measurement. Also, the connection of the components to the operational amplifier is very important. It is a good idea to double or triple check the construction of the amplifying circuits.

In order to reduce the time it would take to gather data, it was beneficial to have all four circuits built before starting to collect data. Thus one would be able to keep the temperature at steady state and switch circuits rather than keep the same circuit and change temperature (in the previous method the cost is somewhat higher than the latter one but time would be reduced significantly) . With that said, the Voltage Mode and the Current Mode were constructed on the same breadboard as seen in Figure 9.
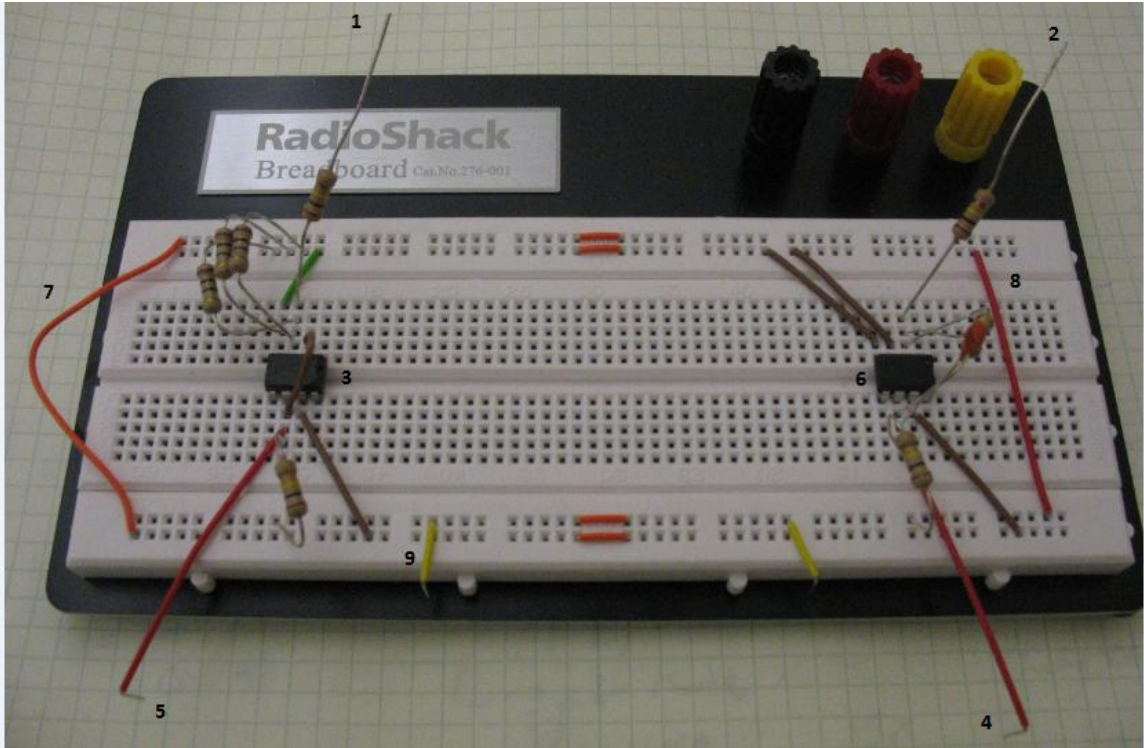
Figure 10. Setup for amplifying circuits for the Voltage Mode (left) and Current Mode (right).

The numbers in this figure represent the following:

1. Signal input to the Voltage Mode

2. Signal input to the Current Mode

3. Operational amplifier for Voltage Mode

4. Signal output for Current Mode

5. Signal output for Voltage mode

6. Operational amplifier for Current Mode

7. The connection of the positive end of the DC power supply. Red wire connects the positive end to both sides of the breadboard.

8. The connection of the negative end of the DC power supply.

9. Ground connection for oscilloscope connection.

A different electrical breadboard and components were used to construct the modified Wien Oscillator and the double Current Mode circuits. A representation of these two amplifying circuits is shown in Figure 10 (modified Wien Oscillator-left, and double Current Mode-right). The list given for Figure 9 applies to Figure 10 except the Voltage Mode is replaced by the modified Wien Oscillator and the Current Mode is replaced with the double Current Mode.
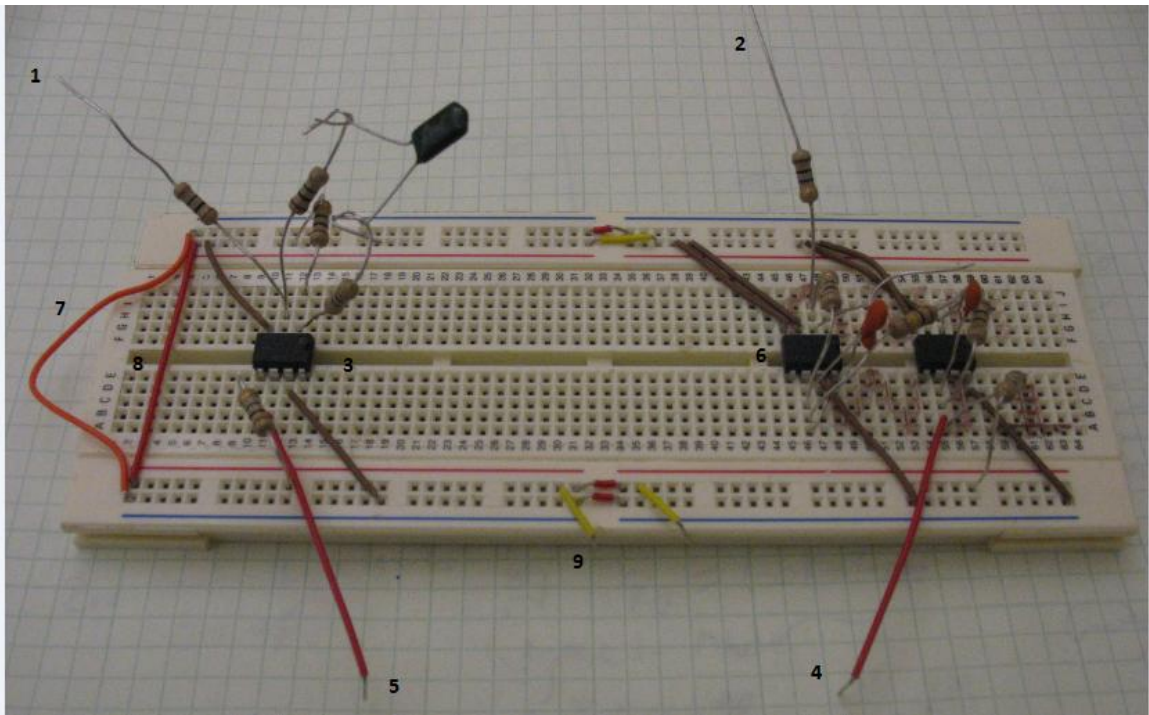
Figure 11. Setup for amplifying circuits for a modified Wien Oscillator circuit (left) and double Current Mode (right).

With the circuits completed, the next step was to the setup of the enclosure and the components inside it. This setup is only pertinent for temperature measurements above the room temperature (23°C in this case). The reason behind choosing the enclosure was to keep the sensor, the heater, and the thermocouple in the same place such that any extraneous heating or cooling effects on the sensor would be negligible. Moreover, an enclosed space small

enough such that its volumetric temperature would change rapidly and reach steady state faster was necessary. This is important because it saves a great deal of time. As mentioned in the previous section, a small enclosure with a volume of 20 in^3 was chosen and was well insulated. The lithium tantalate sensor and a thermocouple attached to its side (with the measuring end of the thermocouple not touching the sensor) were placed inside the enclosure. Across from them, at a distance of ~2 inches, the silicon rubber heater was placed. The senor output was then connected through copper wires to the ground and to the signal input of the amplifying circuits. The heater was powered by the AC power source mentioned in the previous section and the thermocouple was connected to a digital thermometer. A diagram of the complete setup is given below.
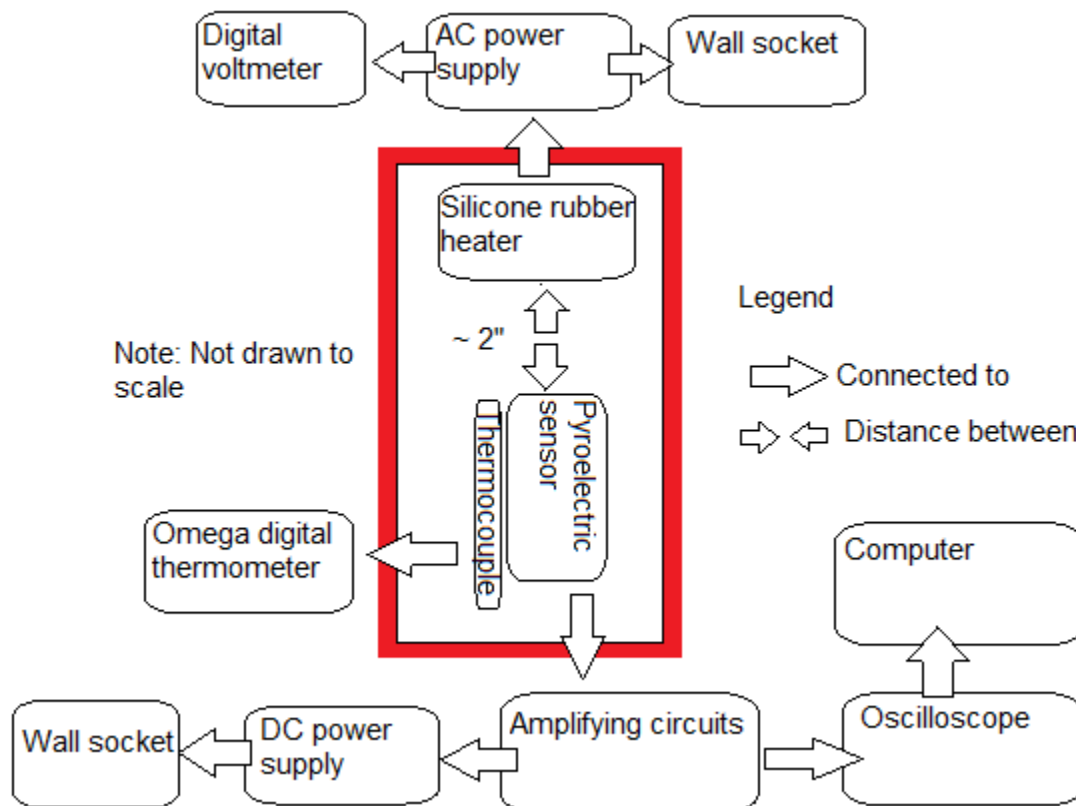
Figure 12. Diagram of the experimental setup.

The enclosure used for temperature measurements below room temperature was a small refrigerator with an area of 1.7 ft^3. The pyroelectric sensor and the thermocouple were enclosed in a plastic wrapping to reduce condensation and similarly the wire connections were insulated by means of electrical tape for the similar reasons.

With the enclosures and the amplifying circuits completed, the experimental setup was almost complete. To better understand the experimental setup Figure 11 is displayed below.
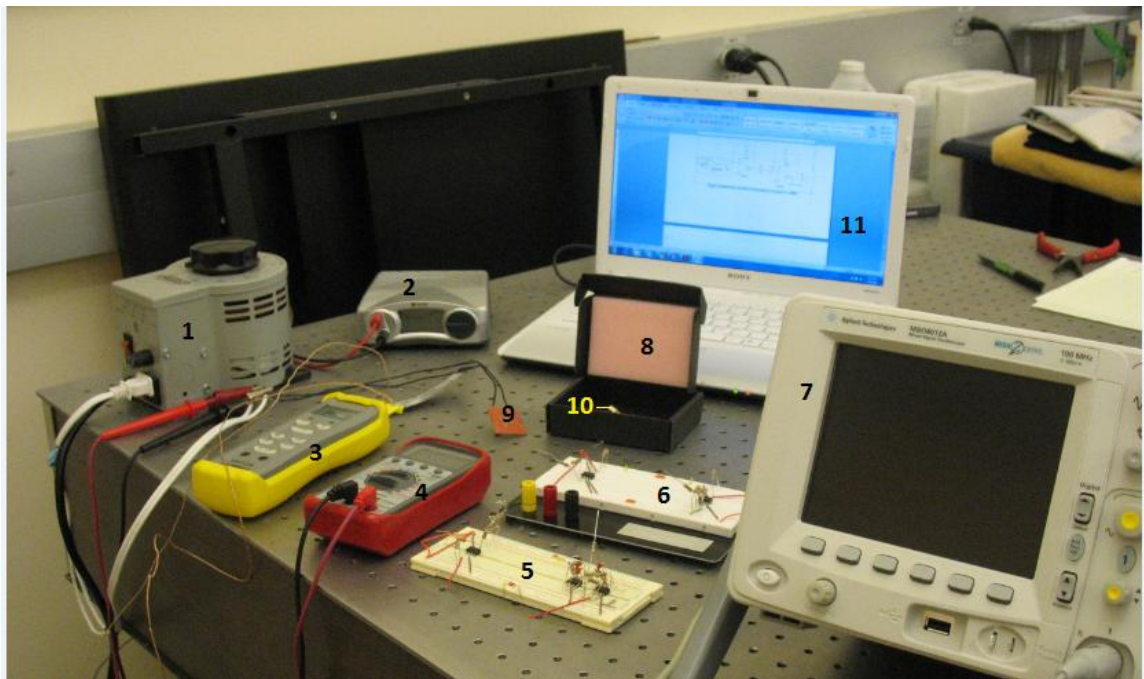
Figure 13. The components and the experimental setup for thermal response of lithium tantalate.

In this picture all the necessary instrumentations are shown with the exception of the small refrigerator. The numbered instruments and components are the following:

1. AC power supply
2. DC power supply

3. Digital thermometer

4. Digital Voltmeter

5. Breadboard consisting of the modified Wien Oscillator and the double Current Mode

6. Breadboard consisting of the Voltage Mode and Current Mode

7. Oscilloscope

8. Enclosure

9. Silicon rubber heater

10. Lithium tantalate pyroelectric sensor

11. Sony Vaio personal laptop for recording the data

The parts listed above are connected in the following fashion. The lithium tantalate sensor, silicon rubber heater, and the thermocouple are placed inside the enclosure. The thermocouple is connected to the digital thermometer. The heater is powered by the AC source and the power input to the heater is monitored by a digital voltmeter. The sensors output signal is connected to the input of the amplifying circuit. The DC power supply is connected to the breadboard and the output signal of the amplifying circuit on the breadboard is connected to the oscilloscope. The oscilloscope's output then is recorded in Microsoft Office Excel 2007.

The procedure for temperature measurement is as follows:

1. Construct the amplifying circuits

2. Construct the enclosure

3. Connect everything as mentioned in the paragraph above

4. Connect the sensor to the desired amplifying circuit's input

5. Turn on everything

6. Set the DC power source to the desired voltage

7. Connect the oscilloscope to the ground and to the output of the desired amplifying circuit

8. Set the oscilloscope to "AutoFit"

9. Set the oscilloscope to measure "Maximum Voltage" and "Minimum Voltage"

10. Take 10 measurements each at a minute apart and record the data.

11. Repeat step 9 for the rest of the circuits and record the data

12. Take the mean and the standard deviation of the data

13. Increase the AC power supply until the desired temperature inside the enclosure is reached

14. Wait 30 minutes and make sure the temperature does not change in order to assume steady state temperature

15. Repeat steps 7-14 for all desired temperature measurements

16. For measurements below room temperature, repeat steps 1-15 using the small refrigerator in lieu of the heater.

This step-by-step process of data collection is the conclusion of the materials and methods chapter. It is important to mention that the standard deviation and the mean of the ten data points are necessary for data interpretation.

CHAPTER 4: RESULTS AND DISCUSSION

4.1: Theoretical Expectations

Lang et al. (1969) has studied the use of a pyroelectric sensor in parallel with a shunt resistor. The figure below shows the circuit which is studied by them. The emphasis is put on the importance of the shunt resistor R_s.
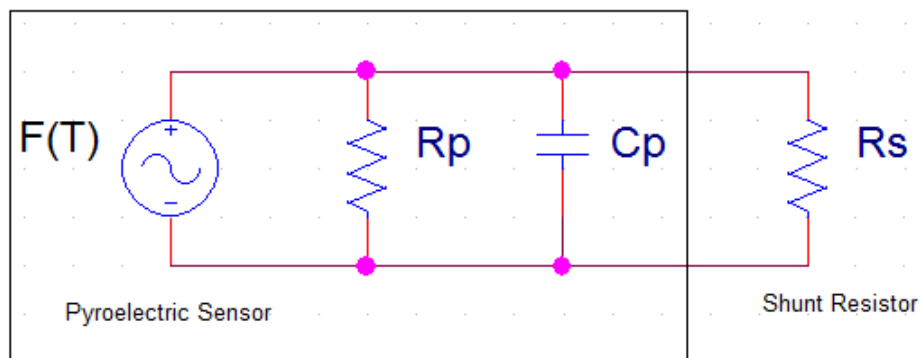
Note: Reproduced fro Lang et al. (1969).
Figure 14. Circuit studied by Lang et al. (1969).

For this thesis, this type of configuration was used as part of the Voltage Mode and modified Wien Oscillator amplifying circuits but not for the Current Mode and the double Current Mode as simulated results show higher slopes for the voltage output for the former amplifying circuits.

There are three cases on how the shunt resistor affects the voltage vs. time curve. The first is when $R_s << R_p$ the second case is when $R_s \geq R_p$ and the third case is when $R_s = R_p$. The graphs for arbitrary units for voltage vs. time are given below.
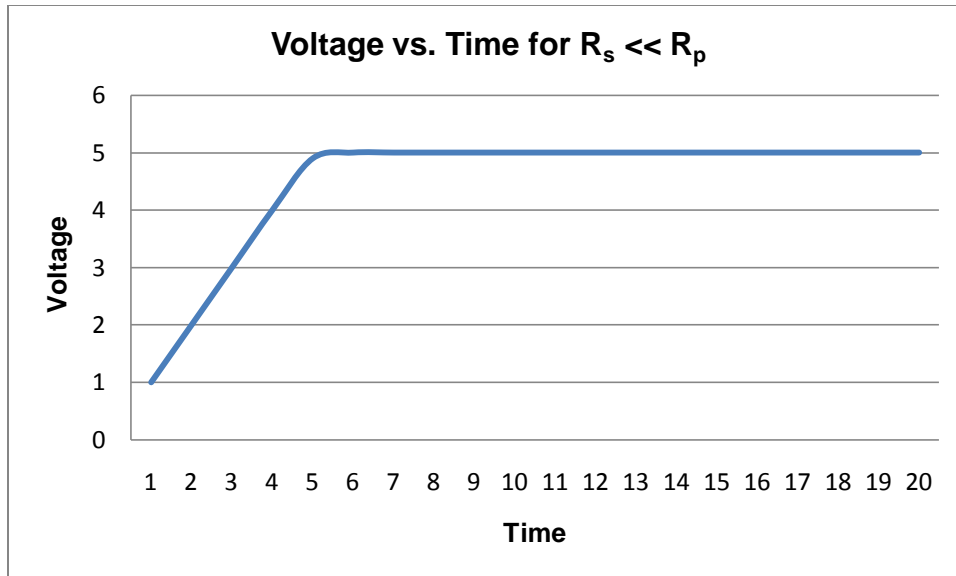
Figure 15. Voltage vs. time for shunt resistor value much lower than pyroelectric resistance.
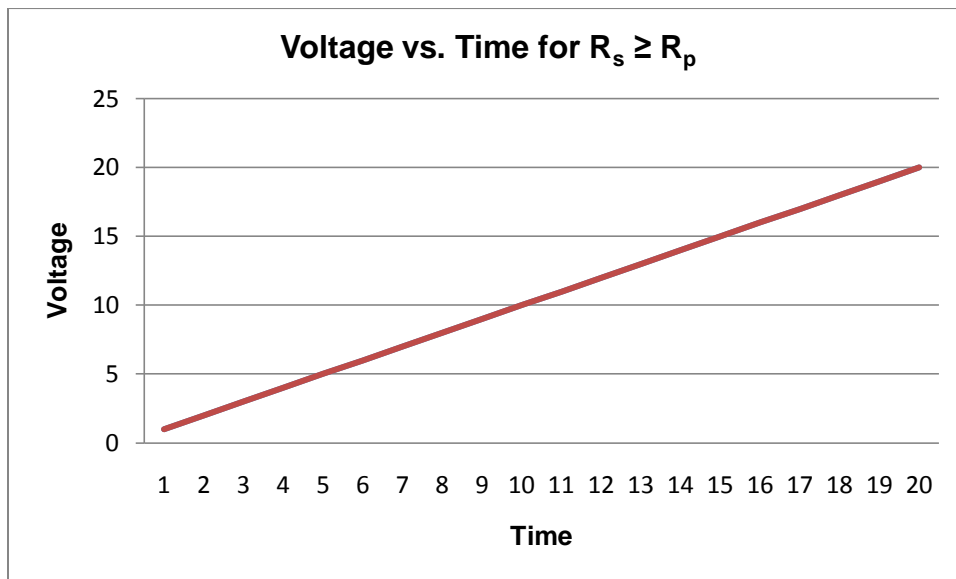
Figure 16. Voltage vs. time for shunt resistace higher or equal to the pyroelectric resistance.
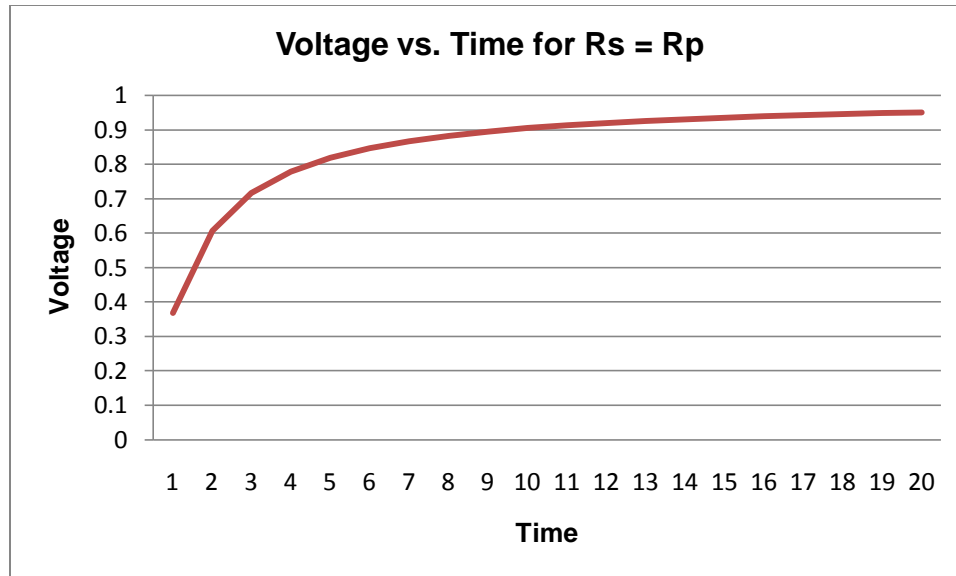
Figure 17. Voltage vs. time for shunt resistance equal to the pyroelectric resistance.

Because the pyroelectric resistance of the sensor used for this thesis is in the

order of >10^12 ohms and the shunt resistances are in the order of 10^5 ohms, it

was expected for the voltage response with time to follow the form seen in Figure

15. Since the sensor is allowed to reach steady state, the voltage output at a

certain temperature was expected remain the same with time. The voltage output

should only change with a change in temperature. Moreover, this behavior

should be expected for the two circuits which are implementing the shunt

resistor: Voltage Mode and modified Wien Oscillator. As mentioned above, the

shunt resistor was used for these two amplifying circuits because the simulation

using OrCAD and PSpice showed higher slopes for them as compared to other

two. On the other hand, the Current Mode and the double Current Modes should

be expected to follow the form given on the figure below due to the fact that no

shunt resistor is present. Lack of a shunt resistor would cause the voltage output

with time to reach a peak then decay to zero with time. Thus, the voltage output

for these two amplifying circuits would be expected to follow a linear behavior

with a slope closer to zero unlike the Voltage or the Wien Oscillator modes.
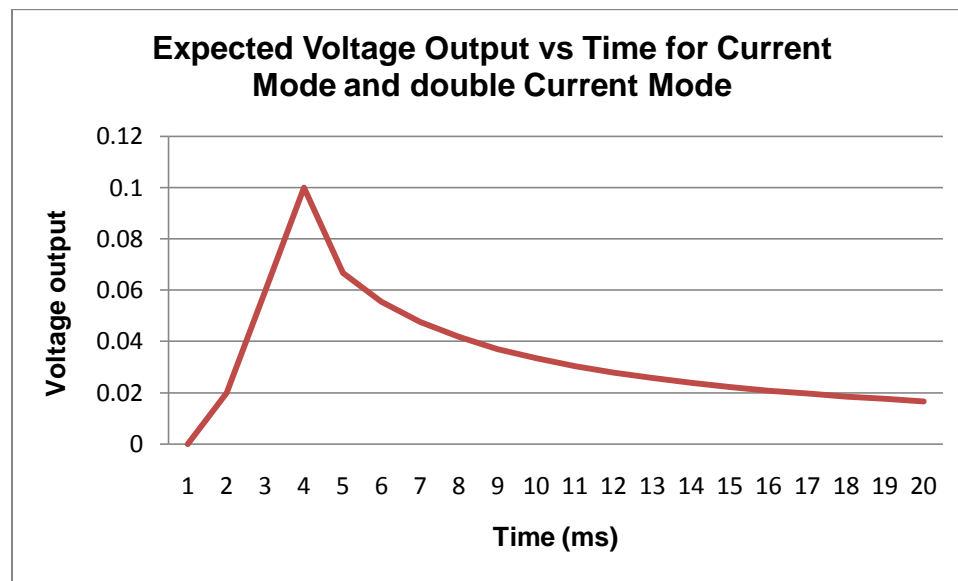
Note: Reproduced from Tuoayar (2007).
Figure 18. Response of voltage output vs. time for the Current Mode and double Current Mode.

OrCAD Family 9.2 Capture CIS Lite Edition and PSpice were used to simulate

the correlation between the current generated by the sensor and the voltage

output. This allows comparisons to be made between theoretical and

experimental results.

4.2: Experimental Results

As mentioned in the previous chapter, all temperature measurements

were taken at steady state. If the temperature of the enclosure did not change for

thirty minutes, this was assumed as achieving steady state. After the latter was

reached, ten measurements of the minimum voltage and maximum voltage were

taken at one minute intervals. These measurements were recorded in Microsoft

Office Excel 2007. The mean and standard deviation of all the measurements

were calculated using Excel. In this case, the standard deviation of the ten measurements taken is the only statistical method necessary to describe the behavior of the data. The voltage output from the sensor was measured at sixteen different temperatures (5, 10, 15, 23, 31, 36, 41, 47, 53, 60, 67, 73, 80, 87, 94, and 99°C). The ten measurements which were taken at each temperature were also taken for each of the four amplifying circuits. After the measurements were made and recorded, the averages at each temperature were calculated and plotted. Out of eight possibilities (maximum voltage and minimum voltage for all four circuits) three demonstrated linear behavior with noticeable slopes and the rest exhibited linear behaviors with slopes close to zero. The three modes which exhibited linear behavior were the measurements for the maximum voltage and minimum voltage of the modified Wien Oscillator and the maximum voltage for the Voltage mode.

Table 10 displays the V_{max} (maximum voltage) average the standard deviation for all temperatures for the modified Wien Oscillator. From this table, a linear behavior of the voltage maximum throughout the temperature range is observed. Moreover, the standard deviation has a range between 0.5 and 1.0mV. This plays a big role on how useful this data could be. To understand the importance of the standard deviation we must take a look at the plot of the maximum voltage against temperature which is given in Figure 19. As can be seen the data is linear with a slope of 2.12736mV. The slope in this case represents the resolution of the collected data. We are getting a response of 2.12736mV/^{o}C with a standard deviation between 0.5 and 1mV.

Table 10. Mean and standard deviation of the ten V_{max} measurements at each temperature for the modified Wien Oscillator amplifying circuit.

Temperature (^oC)	Mean (V)	Standard Deviation (V)
5	1.4182	0.000788811
10	1.4297	0.000823273
15	1.4424	0.000699206
23	1.4623	0.00082327
31	1.4828	0.000632456
36	1.5034	0.000843274
41	1.5208	0.000918937
47	1.5329	0.000875595
53	1.5408	0.000918937
60	1.5522	0.000918937
67	1.5621	0.000567646
73	1.5753	0.000823273
80	1.5872	0.000632456
87	1.5981	0.000875595
94	1.61	0.000666667
99	1.6203	0.000674949

Moreover, the correlation coefficient for this data is R^2=0.9823 with R^2=1 being a perfect correlation of the data. This means that all the data has an almost perfect linear dependence. With the standard deviation being smaller than the resolution and the linear dependence of the data almost perfect, we could say the maximum voltage measurement for the modified Wien Oscillator could be used for temperature measurement for this temperature range.
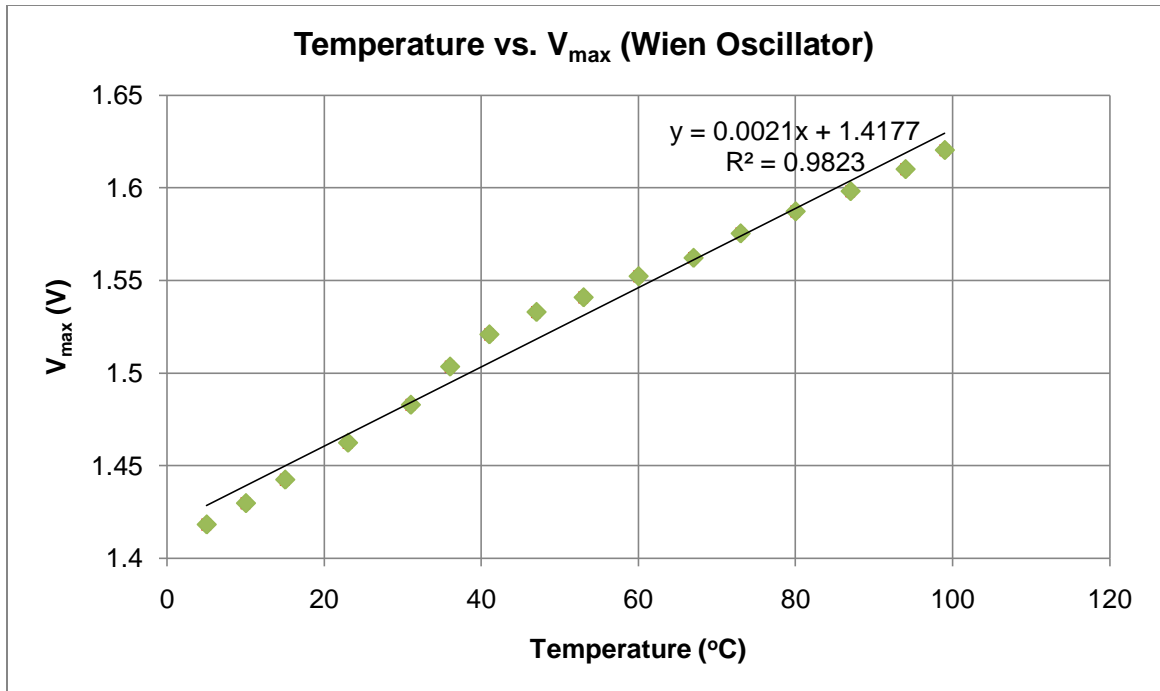
**Figure 19. The average maximum voltage vs. temperature
for the modified Wien Oscillator with error bars of one standard deviation
in each direction vertically and 0.5°C in each direction horizontally.**

Similarly, Table 11 shows the V_{min} average and the standard deviation for

the modified Wien Oscillator mode and Figure 20 shows a plot of this data.

Correspondingly, the standard deviation of this data has a range between 0.5

and 1mV and the linear dependence of the data is R^2=0.9929. The slight

difference between the maximum voltage and minimum voltage for the modified

Wien Oscillator mode is the slope or resolution. The resolution is slightly higher

for the maximum voltage (0.2021mV) with the resolution of the V_{min} graph being

1.92526mV. Furthermore, the minimum voltage has a slightly better linear

dependence than the maximum voltage. Either quantity could very easily be used

for temperature measurement of temperatures between freezing and boiling

points of water.

Table 11. Mean and standard deviation of the ten V_{min} measurements at each temperature for the modified Wien Oscillator amplifying circuit.

Temperature (^{o}C)	Average (V)	Standard Deviation (V)
5	1.1875	0.000849837
10	1.1981	0.000737865
15	1.2101	0.000567646
23	1.2218	0.000788811
31	1.2475	0.000849837
36	1.2606	0.000843274
41	1.2718	0.000918937
47	1.2817	0.000823273
53	1.2918	0.000918937
60	1.3	0.000632456
67	1.3161	0.000875595
73	1.3261	0.0005
80	1.341	0.000666667
87	1.3543	0.000823273
94	1.3616	0.000843274
99	1.3704	0.000699206

Temperature vs. V_{min} (Wien Oscillator)

$y = 0.002x + 1.1835$
$R^2 = 0.9929$

Figure 20. The minimum voltage measured vs. temperature for the modified Wien Oscillator with error bars of one standard deviation in each direction vertically and 0.5^{o}C in each direction horizontally.

Equally, Table 12 and Figure 21 show the V_{max} data for the Voltage mode. Similar to the two previous measurements, there is a linear dependence of this data with a correlation coefficient of $R^2=0.9952$. This linear dependence is the best out of all three modes, but there is a disadvantage to this mode compared to the other ones. The resolution or the slope of this data is almost half of the resolution of the modified Wien Oscillator at 0.99053mV. The standard deviation of the data is similar to the other two measurements. Although this method could be used for temperature measurement in the range specified above, it could be misleading since the slopes and the standard deviations of the data sets are almost the same.

Table 12. Mean and standard deviation of the ten V_{max} measurements at each temperature for the Voltage Mode amplifying circuit.

Temperature (°C)	Average (V)	Standard Deviation (V)
5	0.4923	0.000823273
10	0.4951	0.000737865
15	0.5026	0.000516398
23	0.5081	0.000737865
31	0.5149	0.000737865
36	0.5209	0.000737865
41	0.5236	0.000516398
47	0.5279	0.000875595
53	0.5347	0.000823273
60	0.5415	0.000849837
67	0.5499	0.000875595
73	0.5579	0.000875595
80	0.566	0.000942809
87	0.5719	0.000737865
94	0.579	0.000666667
99	0.5864	0.000516398
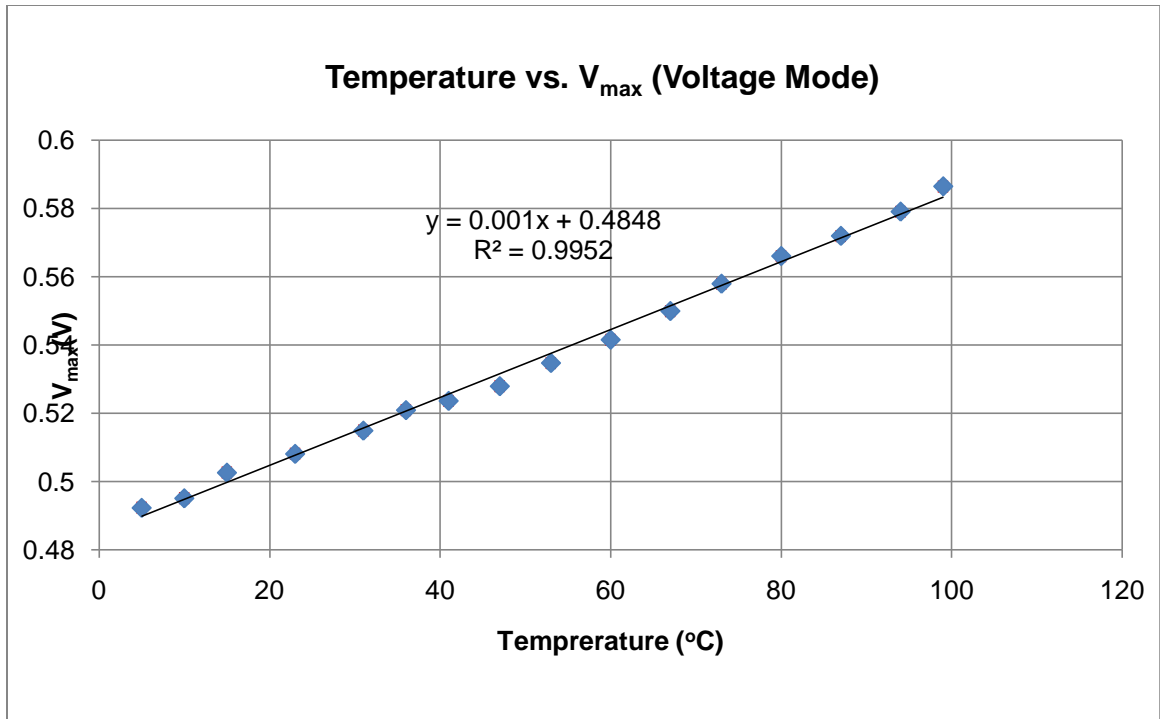
**Figure 21. The maximum voltage measured vs. temperature
for the Voltage Mode with error bars of one standard deviation in each direction
vertically and 0.5°C in each direction horizontally.**

For the Current Mode and double Current Mode, the tables and graphs

are given below. As expected, they have linear behaviors with slopes of nearly

zero for the temperature range. Moreover, the correlation coefficients for the

graphs are very low with R^2=0.4077. The voltage output and the standard

deviation for the double Current mode is twice that of the Current Mode. The

standard deviation for both circuits is much larger than the resolution (slope of

the line) thus these two circuits cannot be used for temperature measurement.

Table 13. Mean and standard deviation of the ten V_{max} measurements at each temperature for the Current Mode amplifying circuit.

Temperature (^oC)	Average (V)	Standard Deviation (V)
5	0.4869	0.000875595
10	0.487	0.000816497
15	0.4881	0.000875595
23	0.487	0.000816497
31	0.4878	0.000918937
36	0.4874	0.000843274
41	0.4868	0.000918937
47	0.486	0.000471405
53	0.4863	0.000948683
60	0.4863	0.000823273
67	0.486	0.000942809
73	0.4861	0.000994429
80	0.4864	0.000699206
87	0.4861	0.000994429
94	0.4866	0.000966092
99	0.4865	0.000971825
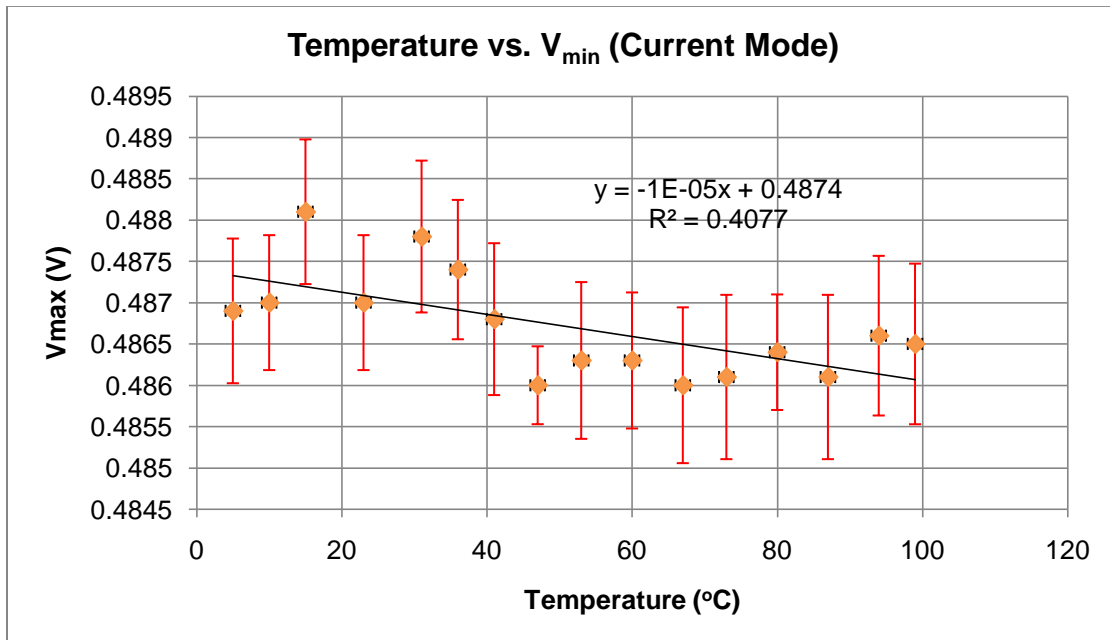
Figure 22. The maximum voltage measured vs. temperature for the Current Mode with error bars of one standard deviation in each direction vertically and 0.5^oC in each direction horizontally.

Table 14. Mean and standard deviation of the ten V$_{max}$ measurements at each temperature for the double Current Mode amplifying circuit.

Temperature (^{o}C)	Average (V)	Standard Deviation (V)
5	0.9738	0.00175119
10	0.974	0.001632993
15	0.9762	0.00175119
23	0.974	0.001632993
31	0.9756	0.001837873
36	0.9748	0.001686548
41	0.9736	0.001837873
47	0.972	0.000942809
53	0.9726	0.001897367
60	0.9726	0.001646545
67	0.972	0.001885618
73	0.9722	0.001988858
80	0.9728	0.001398412
87	0.9722	0.001988858
94	0.9732	0.001932184
99	0.973	0.001943651

Temperature vs. V$_{max}$ (double Current Mode)
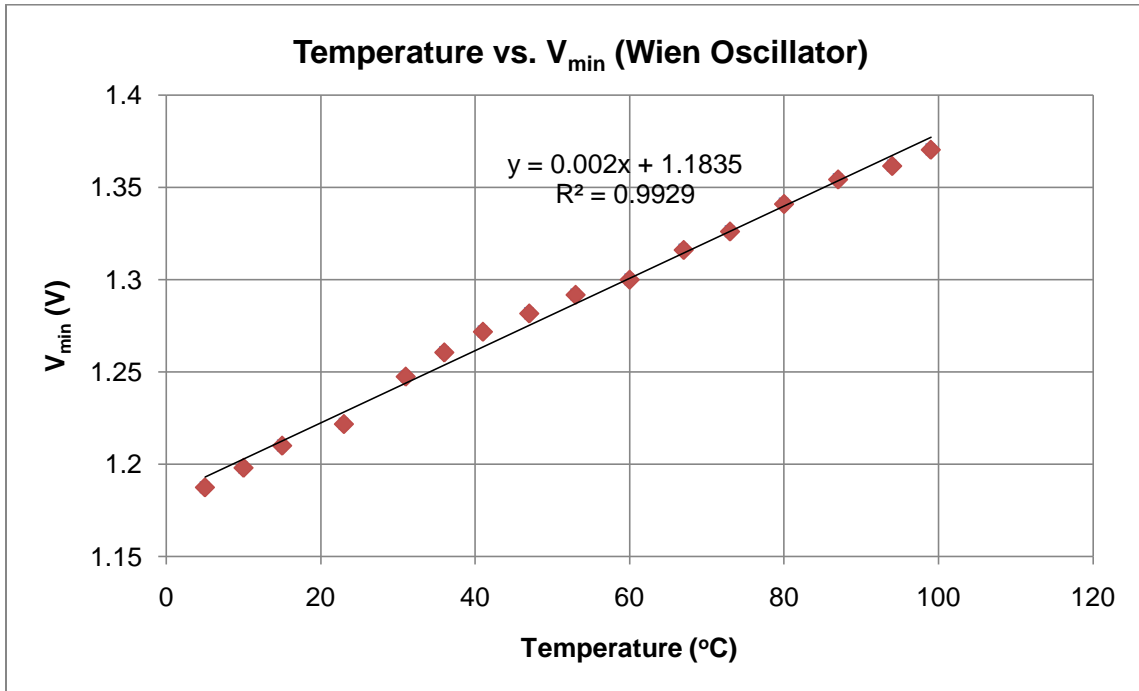
$y = -3E-05x + 0.9748$
$R^{2} = 0.4077$
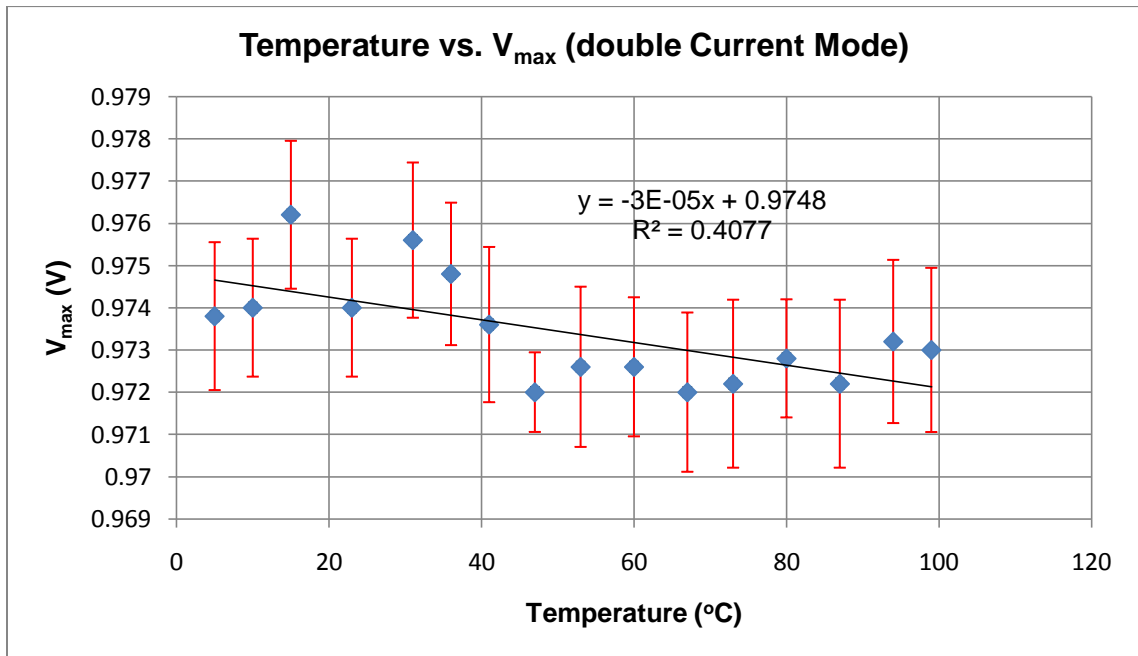
Figure 23. The maximum voltage measured vs. temperature for the Double Current Mode with error bars of one standard deviation in each direction vertically and 0.5^{o}C in each direction horizontally.

Moreover, 90% and 95% confidence intervals are given for the ten measurements at each temperature for all the amplifying circuits. These confidence intervals are given in Appendix C on Table 15 and Table 16 for 90% and 95% respectively. For the Wien Oscillator the values for a 95% CI are on average at 0.553mV and for a 90% CI are on average 0.484mV. With the slope of the data for the Wien Oscillator being at 2.12736mV, it is observed that the range of the voltage output at a certain temperature deviates by 0.484mV with 90% confidence and by 0.553mV with a 95% confidence. This shows that all measurements are three to four times smaller than the slope of the line at both confidence intervals thus allowing for an accurate temperature measurement for this mode. Similarly, the Voltage Mode has a slope of 0.99053mV and the confidence interval values at 95% and 90% are 0.615mV and 0.464mV respectively. This also implies that no data is larger than the slope thus allowing for accurate temperature measurement although it is not as accurate as the Wien Oscillator.

On the other hand, the Current Mode and the double Current Mode have slopes much smaller than the confidence interval values. This shows that the error is too large for each temperature thus neither amplifying circuit could be used for temperature measurement.

These tables and figures conclude the results chapter. It has been shown that all three modes (modified Wien Oscillator V_{max} and V_{min} and Voltage Mode V_{max}) have linear dependence with a high enough slope to be measurable by modern voltage measuring devices. All data compare well to the graphs given by

Capture CIS Lite Edition from the OrCAD Family 9.2. These graphs are shown

below in Figure 24 and Figure 25 and correspond to the slope of the voltage

output expected for the Voltage Mode and for the modified Wien Oscillator

respectively. The slope of the voltage output is taken as a function of the

expected values of the current generated by the sensor between 0-100°C (0-1

micro ampere). It could be expected to see a slope of 1mV/$^{\circ}$C for the voltage

mode and a slope of 2mV/$^{\circ}$C for the modified Wien Oscillator. The total change

in voltage output for the temperature range should be ~94mV for the Voltage

Mode and ~188mV for the modified Wien Oscillator. Both these values are

comparable to the V_{99}-V_5 for both the Voltage Mode (0.5864-0.4923=94.1mV)

and the modified Wien Oscillator (1.6203-1.4182=202.1mV for V_{max} and

1.3704-1.1875= 182.9mV for V_{min}).
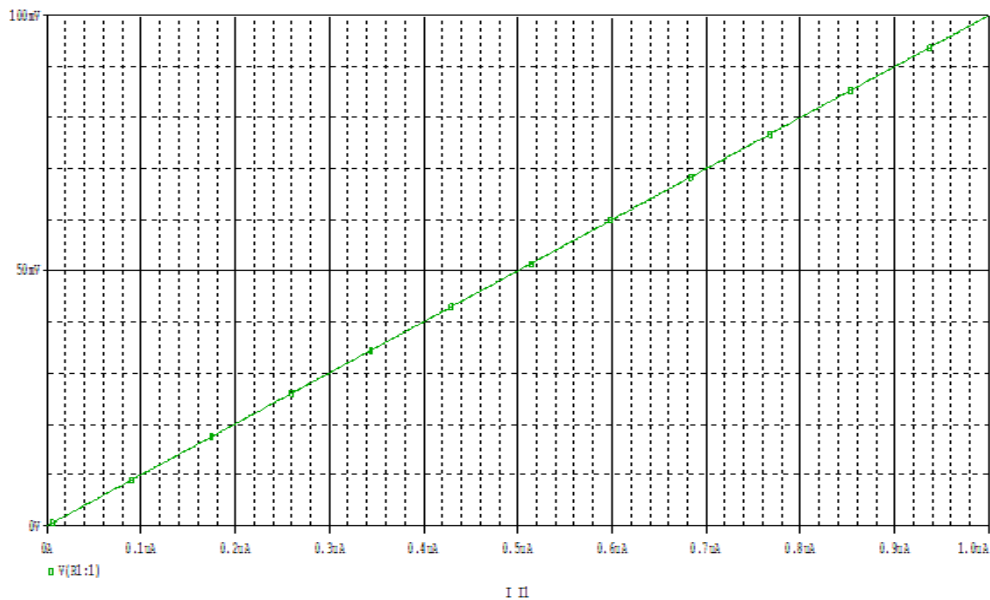
**Figure 24. The expected slope of the voltage output using the
Voltage Mode amplifying circuit generated with
OrCAD 9.2 Capture CIS Lite Edition and PSpice.**
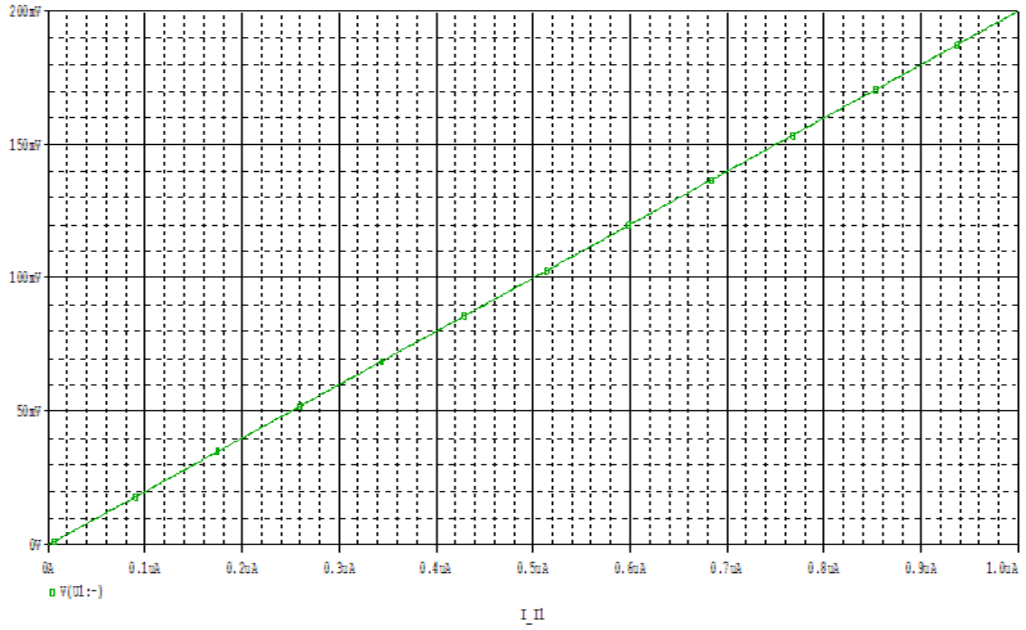
Figure 25. The expected slope of the voltage output using the modified Wien Oscillator amplifying circuit generated with OrCAD 9.2 Capture CIS Lite Edition and PSpice.

CHAPTER 5: CONCLUSION AND SUGGETIONS

In this thesis, a study of the thermal response of lithium tantalate for temperature measurement purposes was presented. The pyroelectric sensor, containing the lithium tantalate material, was subjected to temperatures between 5-99$^{\text{o}}$C and the voltage response was measured at sixteen different temperatures within that range. Four different amplifying circuits were used for signal amplification since the current output of such a sensor is in the order of nano-micro amperes. Ten measurements were taken at steady state at a certain temperature for each different amplifying circuit. The maximum and minimum voltages were measured for each circuit using an oscilloscope. The average and standard deviation of these ten points were calculated using Microsoft Excel 2007. The averages were then plotted against temperature to identify correlations. Three modes showed linear relationships (maximum and minimum voltage for modified Wien Oscillator and maximum voltage for Voltage Mode). The rest did not show any correlation. Both modes using the modified Wien Oscillator displayed a nearly perfect linear dependence with a resolution of approximately 2.1mV/$^{\text{o}}$C. The voltage mode showed similar results for linear dependence, but the resolution was half that of the modified Wien Oscillator. Moreover, all three modes had standard deviations between 0.5 and 1mV. It could be said that the modified Wien Oscillator mode is more appropriate for temperature measurement for this temperature range.

The experimental results compare well with the theoretical results computed using OrCAD 9.2 Capture CIS Lite Edition. For the temperature range which was studied, both the experimental and theoretical data display an increasing slope of about 2mV/^{o}C for the modified Wien Oscillator and 1mV/^{o}C for the Voltage Mode. Because their linear dependence is almost perfect and their resolutions are measurable with devices we have today, it is reasonable to assume that the measurement of temperatures between freezing and boiling points of water is possible.

The resolution of the data could be improved using different values for the components of the amplifying circuits. Different values give different outputs and thus there are values which optimize the resolution. Moreover, the standard deviation of the data could be improved by reducing the input voltage to the electrical breadboard and by eliminating fluctuations of the frequency at which the heating and cooling devices are running. In addition, better test equipment would improve the overall data collection process and eliminate any other errors which may occur along the way.

The modified Wien Oscillator amplifying circuit has not been used in any previous work concerning the amplification of pyroelectric signals. Future studies are possible using such a circuit for amplification of pyroelectric signals for different applications.

REFERENCES

Batra, A. K., Aggarwal, M. D., Edwards, M. E., & Bhalla, A. (2008). Present Status of Polymer: Ceramic Composites for Pyroelectric Infrared Detectors. *Ferroelectrics* , 84-121.

Batra, A. K., Guggilla, P., Currie, J. R., Aggarwal, M. D., & Alim, M. A. (2006). Pyroelectric Ceramics for Infrared Detection Applications. *Materials Letters* , 1937-1942.

Chirtoc, M., Bentefour, E. H., Antoniow, J. S., Glorieux, C., Thoen, J., Delenclos, S., et al. (2003). CUrrent Mode Versus Voltage Mode Measurement of Signals From Pyroelectric Sensors. *Review of Scientific Instruments* , 648-650.

Chung, W. Y., Sun, T. P., & Kao, Y. L. (1996). Design of Pyroelectric IR Readout Circuit Based on $LiTaO_3$ Detectors. *1996 IEEE International Symposium on Circuits and Systems. Circuits and Systems Connecting the World* , 225-228.

Chvatal, M., Sedlakova, V., & Majzner, J. (2009). Noise Analysis of Infrared Detectors. *2009 32nd International Spring Seminar on Electronics Technology. Hetero System Integration, the Path to New Solutionsin the Modern Electronics*, (p. 3).

Cuadras, A., Gasulla, M., & Ferrari, V. (2010). Thermal Energy Harvesting Through Pyroelectricity . *Sensors and Actuators, A: Physical* , 132-139.

DeWitt, D. P., & Nutter, G. D. (1988). *Theory and Practice of Radiation Thermometry.* New York: J. Wiley & Sons.

Dietze, M., Krause, J., Solterbeck, C. H., & Es-Souni, M. (2007). Thick Film Polymer-Ceramic Composites for Pyroelectric Applications. *Journal of Applied Physics* , 54113-1-7.

Epstein, R. I., & Malloy, K. J. (2009). Electrocaloric Devices Based on Thin-Film Heat Switches. *Journal of Applied Physics* , 064509-7.

Fedosov, S. N., & Von Seggern, H. (2008). Pyroelectricity in Polyvinylidene Fluoride: Influence of Polarization and Charge. *Journal of Applied Physics*, 014105-1-8.

Fukada, E. (1989). Introduction: Early Studies in Piezoelectricity, Pyroelectricity, and Ferroelectricity in Polymers . *Phase Transitions* , 135-141.

Guyomar, D., Sebald, G., Pruvost, S., & Lallart, M. (2009). Energy Harvesting From Ambient Vibrations and Heat. *Journal of Intelligent Material Systems and Structures* , 609-624.

Jacob, M. V., Hartnett, J. G., Mazierska, J., Giordano, V., Krupta, J., & Tobar, M. E. (2004). Temperature Dependence of Permittivity and Loss Tangent of Lithium Tantalate at Microwave Frequencies. *IEEE Transaction on Microwave Theory and Techniques* , 536-541.

Kao, K. C. (2004). *Dielectric Phenomena in Solids.* Academic Press.

Kinzie, P. A. (1973). *Thermocouple Temperature Measurement.* New York: J. Wiley.

Kohli, C. H., Schmid, P. E., & & Levy, F. (1998). Electrical and Pyroelectric Properties of Lithium Tantalate Thin Films . *Ferroelectrics* , 471-482.

Lang, S. B. (2004). A 2400 Year History of Pyroelectricity: From Ancient Greece to Exploration of the Solar System. *British Ceramic Transactions* , 65-70.

Lang, S. B. (1981). Bibliography on Piezoelectricity and Pyroelectricity of Polymers. *Ferroelectrics* , 191-245.

Lang, S. B. (2005). Pyroelectricity: From Ancient Curiosity to Modern Imaging Tool. *Physics Today* , 31-36.

Lang, S. B. (1974). *Sourcebook of Pyroelectricity.* New York: Gordon and Breach Science Publishers.

Lang, S. B. (1999). The History of Pyroelectricity: From Ancient Greece to Space Missions. *Ferroelectrics* , 99-108.

Lang, S. B., Shaw, S. A., Rice, L. H., & Timmerhaus, K. D. (1969). Pyroelectric Thermometer for Use at Low Temperatures. *The Review of Scientific Instruments* , 274-284.

Lau, S. T., Cheng, C. H., Choy, S. H., & Lin, D. M. (2008). Lead-Free Ceramics for Pyroelectric Applications. *Journal of Applied Physics* , 014105-1-4.

Li, S., Wu, X., Zhang, L., & Yao, X. (2008). Study of Poling Methods for Multilayer Pyroelectric Thin Film for Infrared Detectors. *Journal of Electroceramics* , 520-523.

Lovinger, A. J. (1983). Ferroelectric Polymers. *Science* , 1115-1121.

Malhame, R. P. (2002). Elementary Amplitude and Distortion Evaluation in Wien and Phase Shift Oscillators. *ICM 2002. 14th International Conference on Microelectronics* , 140-143.

McGee, T. D. (1988). *Principles and Methods of Temperature Measurement.* New York: J. Wiley & Sons.

Michalski, L., Eckersdorf, K., Kucharski, J., & McGhee, J. (2001). *Temperature Measurement.* New York: J. Wiley.

Mischenko, A. S., Zhang, Q., Scott, J. F., & Whatmore, R. W. (2008). A New Approach to Interconversion of Thermal and Electrical Energy. *2006 8Th International Conference on Solid-State and Integrated Circuit Technology*, (pp. 1-4).

Nalwa, H. S. (1995). *Ferroelectric Polymers: Chemistry, Physics, and Applications.* New York: Marcel Dekker.

Norkus, V., Schulze, A., Querner, Y., & Gerlach, G. (2010). Thermal Effects to Enhance the Responsivity of Pyroelectric Infrared Detectors. *Procedia Engineering 5* , 944-947.

Nougaret, L., Combette, P., & Pascal-Delannoy, F. (2009). Growth of Lithium Tantalate Thin Films by Radio-Frequency Magnetron Sputtering With Lithium Enriched Target. *Thin Solid Films* , 1784-1789.

Plumb, H. H. (1972). *Temperature: Its Measurement and Control in Science and Industry* (Vol. 4). Pittsburgh: American Institute of Physics.

Qiu-Lin, T., Wen-Dong, Z., Chen-Yang, X., & Ji-Jun, X. (2009). Design, Fabrication and Characterization of Pyroelectric Thin Film and Its Appication for Infrared Gas Sensors. *Microelectronics Journal* , 58-62.

Quinn, T. J. (1990). *Temperature.* New York: Academic Press.

Ramos, P., DeAndres, A., & Lopez, S. (2007). Effect of Thermal Losses on the Specific Detectivity of Pyroelectric Infrared Detectors. *Integrated Ferroelectrics* , 147-159.

Safari, A., Panda, R. K., & Janas, V. F. (1996). Ferroelectricity: Materials, Characteristics & Applications. *Key Engineering Materials* , 35-70.

Satapathy, S., Verma, P., Gupta, P. K., Mukherjee, C., Sathe, V. G., & Varma, K. B. (2011). Structural, Dielectric and Ferroelectric Properties of Multilayer Lithium Tantalate Thin Films Prepared by Sol-Gel Technique. *Thin Solid Films* , 1803-1808.

Shaldin, Y. V., Matyjasik, S., Rabadanov, M. K., & Gabrielyan, V. T. (2007). Pyroelectric Properties of Real $LiNbO_3$ Single Crystals. *Doklady Physics* , 579-582.

Shaw, C. P., Whatmore, R. W., & Alcock, J. R. (2007). Porous, Functionally Gradient Pyroelectric Materials . *Journal of the American Ceramic Society*, 138-142.

Smith, B., & Amon, C. (2007). Simultaneous Electrothermal Test Method for Pyroelectric Microsensors. *Journal of Electronic Packaging* , 504-511.

Sokoll, T., Norkus, V., & Gerlach, G. (1997). Ion Beam Etching of Lithium Tantalate and Its Applications for Pyroelectric Linear Arrays. *Surface and Coatings Technology* , 469-474.

Touayar, O., Mellouiki, I., Sifi, N., & Yakoubi, N. (2006). Determination of the Nonequivalence Source Between Electrical and Radiative Heating in a Pyroelectric Sensor Using Experimental Voltage Response and Heat Wave Propagation Theoretical Model. *Sensors and Actuators* , 572-580.

Uchino, K. (2000). *Ferroelectric Devices.* New York: Marcel Dekker.

Vanderpool, D., Yoon, J. H., & Pilon, L. (2008). Simulations of a Prototypical Device Using Pyroelectric Materials for Harvesting Waste Heat. *International Jounral of Heat and Mass Transfer* , 5052-5062.

Whatmore, R. W. (1986). Pyroelectric Devices and Materials. *Report on Progress in Physics* , 1335-1386.

Wong, C. P. (1993). *Polymers for Electronic and Photonic Applications.* Boston: Academic Press.

Xiao, D., & Lang, S. B. (1988). Measurement Applications Based on Pyroelectric Properties of Ferroelectric Polymers. *IEEE Transactions on Electrical Insulation* , 503-516.

Yan, W., Zhang, R., Xiu, X., Xie, Z., Han, P., Jiang, R., et al. (2007). Temperature Dependence of the Pyroelectric Coefficient and the Spontaneous Polarization of AIN. *Applied Physics Letters* , 212102-1-3.

Zhang, Z. M., Tsai, B. K., & Machin, G. (2010). *Radiometric Temeprature Measurements. II. Applications.* Boston: Academic Press.

Zhang, Z. M., Tsai, B. K., & Machin, G. (2010). *Radiometric Temperature Measurements. I. Fundamentals.* Boston: Academic Press.

Zheng, D., Da-Gui, H., & De-Yin, Z. (2008). Thermal Analysis of the Microscale Pyroelectric Thin Film Infrared Detectors. *2008 IEEE International Conference on Mechatronics and Automation*, (pp. 49-54).

APPENDICES

Appendix A: Collected Data for the Voltage Mode (V.M.) and the Modified Wien Oscillator (W.O).

T(^{o}C)	Measurement	V.M. V_{max} (V)	W.O. V_{max} (V)	W.O. V_{min} (V)
5	1	0.492	1.418	1.187
	2	0.493	1.418	1.187
	3	0.493	1.418	1.188
	4	0.492	1.419	1.188
	5	0.492	1.42	1.189
	6	0.494	1.418	1.186
	7	0.491	1.418	1.187
	8	0.492	1.418	1.188
	9	0.492	1.417	1.187
	10	0.492	1.418	1.188
	Mean	0.4923	1.4182	1.1875
	St. Deviation	0.000823273	0.000788811	0.000849837
10	1	0.495	1.429	1.198
	2	0.496	1.43	1.199
	3	0.495	1.43	1.197
	4	0.494	1.431	1.198
	5	0.496	1.431	1.198
	6	0.495	1.43	1.198
	7	0.494	1.429	1.197
	8	0.496	1.429	1.198
	9	0.495	1.429	1.199
	10	0.495	1.429	1.199
	Mean	0.4951	1.4297	1.1981
	St. Deviation	0.000737865	0.000823273	0.000737865
15	1	0.502	1.442	1.21
	2	0.503	1.442	1.21
	3	0.502	1.443	1.211
	4	0.502	1.443	1.21
	5	0.503	1.442	1.21
	6	0.502	1.442	1.21
	7	0.503	1.442	1.21
	8	0.503	1.444	1.211
	9	0.503	1.442	1.21
	10	0.503	1.442	1.209
	Mean	0.5026	1.4424	1.2101
	St. Deviation	0.000516398	0.000699206	0.000567646

23	1	0.509	1.462	1.223
	2	0.509	1.463	1.222
	3	0.507	1.462	1.222
	4	0.508	1.462	1.221
	5	0.509	1.462	1.222
	6	0.508	1.461	1.221
	7	0.508	1.463	1.223
	8	0.508	1.462	1.221
	9	0.507	1.464	1.222
	10	0.508	1.462	1.221
	Mean	0.5081	1.4623	1.2218
	St. Deviation	0.000737865	0.000823273	0.000788811
31	1	0.514	1.483	1.247
	2	0.516	1.483	1.247
	3	0.515	1.483	1.246
	4	0.515	1.483	1.248
	5	0.515	1.482	1.248
	6	0.514	1.482	1.249
	7	0.516	1.483	1.247
	8	0.515	1.484	1.247
	9	0.515	1.483	1.248
	10	0.514	1.482	1.248
	Mean	0.5149	1.4828	1.2475
	St. Deviation	0.000737865	0.000632456	0.000849837
36	1	0.521	1.503	1.261
	2	0.522	1.504	1.262
	3	0.521	1.505	1.262
	4	0.52	1.503	1.26
	5	0.52	1.503	1.26
	6	0.521	1.503	1.26
	7	0.52	1.504	1.26
	8	0.522	1.502	1.26
	9	0.521	1.504	1.261
	10	0.521	1.503	1.26
	Mean	0.5209	1.5034	1.2606
	St. Deviation	0.000737865	0.000843274	0.000843274

41	1	0.524	1.52	1.271
	2	0.524	1.521	1.272
	3	0.524	1.521	1.272
	4	0.523	1.521	1.271
	5	0.523	1.523	1.273
	6	0.524	1.52	1.273
	7	0.524	1.52	1.273
	8	0.523	1.52	1.271
	9	0.524	1.521	1.271
	10	0.523	1.521	1.271
	Mean	0.5236	1.5208	1.2718
	St. Deviation	0.000516398	0.000918937	0.000918937
47	1	0.528	1.532	1.281
	2	0.527	1.533	1.281
	3	0.527	1.534	1.282
	4	0.527	1.532	1.283
	5	0.527	1.532	1.281
	6	0.529	1.532	1.281
	7	0.528	1.533	1.282
	8	0.529	1.533	1.283
	9	0.528	1.534	1.281
	10	0.529	1.534	1.282
	Mean	0.5279	1.5329	1.2817
	St. Deviation	0.000875595	0.000875595	0.000823273
53	1	0.535	1.54	1.292
	2	0.535	1.542	1.291
	3	0.534	1.54	1.293
	4	0.535	1.54	1.292
	5	0.535	1.541	1.292
	6	0.535	1.542	1.291
	7	0.534	1.54	1.29
	8	0.536	1.542	1.292
	9	0.535	1.54	1.292
	10	0.533	1.541	1.293
	Mean	0.5347	1.5408	1.2918
	St. Deviation	0.000823273	0.000918937	0.000918937

Appendix A: (Continued)

60	1	0.541	1.553	1.3
	2	0.542	1.553	1.299
	3	0.541	1.553	1.3
	4	0.543	1.552	1.301
	5	0.543	1.552	1.3
	6	0.541	1.552	1.3
	7	0.541	1.553	1.299
	8	0.541	1.552	1.301
	9	0.541	1.552	1.3
	10	0.541	1.55	1.3
	Mean	0.5415	1.5522	1.3
	St. Deviation	0.000849837	0.000918937	0.000632456
67	1	0.55	1.562	1.315
	2	0.549	1.561	1.316
	3	0.551	1.562	1.316
	4	0.55	1.563	1.316
	5	0.551	1.562	1.315
	6	0.549	1.562	1.317
	7	0.551	1.563	1.316
	8	0.55	1.562	1.316
	9	0.549	1.562	1.318
	10	0.549	1.562	1.316
	Mean	0.5499	1.5621	1.3161
	St. Deviation	0.000875595	0.000567646	0.000875595
73	1	0.558	1.575	1.329
	2	0.556	1.576	1.329
	3	0.558	1.577	1.328
	4	0.559	1.574	1.329
	5	0.558	1.575	1.329
	6	0.558	1.575	1.33
	7	0.559	1.575	1.329
	8	0.557	1.575	1.329
	9	0.558	1.576	1.329
	10	0.558	1.575	1.3
	Mean	0.5579	1.5753	1.3261
	St. Deviation	0.000875595	0.000823273	0.0005

Appendix A: (Continued)

80	1	0.565	1.587	1.341
	2	0.566	1.588	1.34
	3	0.565	1.587	1.34
	4	0.566	1.587	1.342
	5	0.567	1.588	1.341
	6	0.568	1.587	1.341
	7	0.565	1.587	1.342
	8	0.566	1.587	1.341
	9	0.566	1.586	1.341
	10	0.566	1.588	1.341
	Mean	0.566	1.5872	1.341
	St. Deviation	0.000942809	0.000632456	0.000666667
87	1	0.572	1.598	1.354
	2	0.573	1.599	1.354
	3	0.572	1.6	1.355
	4	0.572	1.598	1.355
	5	0.573	1.598	1.356
	6	0.571	1.598	1.354
	7	0.571	1.597	1.353
	8	0.571	1.597	1.354
	9	0.572	1.598	1.354
	10	0.572	1.598	1.354
	Mean	0.5719	1.5981	1.3543
	St. Deviation	0.000737865	0.000875595	0.000823273
94	1	0.579	1.611	1.361
	2	0.579	1.61	1.363
	3	0.58	1.609	1.362
	4	0.58	1.61	1.36
	5	0.578	1.611	1.362
	6	0.579	1.609	1.362
	7	0.579	1.61	1.362
	8	0.579	1.61	1.361
	9	0.579	1.61	1.361
	10	0.578	1.61	1.362
	Mean	0.579	1.61	1.3616
	St. Deviation	0.000666667	0.000666667	0.000843274

Appendix A: (Continued)

99				
	1	0.586	1.62	1.37
	2	0.587	1.621	1.371
	3	0.586	1.619	1.37
	4	0.586	1.62	1.371
	5	0.587	1.62	1.369
	6	0.587	1.621	1.371
	7	0.586	1.621	1.37
	8	0.586	1.62	1.37
	9	0.586	1.621	1.371
	10	0.587	1.62	1.371
	Mean	0.5864	1.6203	1.3704
	St. Deviation	0.000516398	0.000674949	0.000699206

Appendix B: Collected Data for the Current Mode (C.M.) and the Double Current Mode (D.C.M.).

T (^{o}C)	Measurement	C.M. V_{max} (V)	D.C.M. V_{max} (V)
5	1	0.488	0.976
	2	0.487	0.974
	3	0.486	0.972
	4	0.486	0.972
	5	0.488	0.976
	6	0.487	0.974
	7	0.487	0.974
	8	0.486	0.972
	9	0.486	0.972
	10	0.488	0.976
	Mean	0.4869	0.9738
	St. Deviation	0.000875595	0.00175119
10	1	0.487	0.974
	2	0.488	0.976
	3	0.488	0.976
	4	0.488	0.976
	5	0.486	0.972
	6	0.486	0.972
	7	0.487	0.974
	8	0.487	0.974
	9	0.487	0.974
	10	0.486	0.972
	Mean	0.487	0.974
	St. Deviation	0.000816497	0.001632993
15	1	0.488	0.976
	2	0.489	0.978
	3	0.488	0.976
	4	0.487	0.974
	5	0.487	0.974
	6	0.488	0.976
	7	0.489	0.978
	8	0.489	0.978
	9	0.489	0.978
	10	0.487	0.974
	Mean	0.4881	0.9762
	St. Deviation	0.000875595	0.00175119

Appendix B: (Continued)

23	1	0.487	0.974
	2	0.487	0.974
	3	0.488	0.976
	4	0.487	0.974
	5	0.486	0.972
	6	0.486	0.972
	7	0.488	0.976
	8	0.488	0.976
	9	0.487	0.974
	10	0.486	0.972
	Mean	0.487	0.974
	St. Deviation	0.000816497	0.001632993
31	1	0.488	0.976
	2	0.489	0.978
	3	0.489	0.978
	4	0.487	0.974
	5	0.487	0.974
	6	0.487	0.974
	7	0.489	0.978
	8	0.487	0.974
	9	0.487	0.974
	10	0.488	0.976
	Mean	0.4878	0.9756
	St. Deviation	0.000918937	0.001837873
36	1	0.489	0.978
	2	0.488	0.976
	3	0.487	0.974
	4	0.487	0.974
	5	0.488	0.976
	6	0.487	0.974
	7	0.487	0.974
	8	0.488	0.976
	9	0.486	0.972
	10	0.487	0.974
	Mean	0.4874	0.9748
	St. Deviation	0.000843274	0.001686548

Appendix B: (Continued)

41	1	0.486	0.972
	2	0.487	0.974
	3	0.487	0.974
	4	0.486	0.972
	5	0.488	0.976
	6	0.486	0.972
	7	0.486	0.972
	8	0.486	0.972
	9	0.488	0.976
	10	0.488	0.976
	Mean	0.4868	0.9736
	St. Deviation	0.000918937	0.001837873
47	1	0.486	0.972
	2	0.486	0.972
	3	0.486	0.972
	4	0.486	0.972
	5	0.486	0.972
	6	0.485	0.97
	7	0.486	0.972
	8	0.487	0.974
	9	0.486	0.972
	10	0.486	0.972
	Mean	0.486	0.972
	St. Deviation	0.000471405	0.000942809
53	1	0.486	0.972
	2	0.487	0.974
	3	0.487	0.974
	4	0.485	0.97
	5	0.487	0.974
	6	0.486	0.972
	7	0.485	0.97
	8	0.486	0.972
	9	0.488	0.976
	10	0.486	0.972
	Mean	0.4863	0.9726
	St. Deviation	0.000948683	0.001897367

Appendix B: (Continued)

60	1	0.486	0.972
	2	0.486	0.972
	3	0.486	0.972
	4	0.487	0.974
	5	0.485	0.97
	6	0.486	0.972
	7	0.486	0.972
	8	0.486	0.972
	9	0.487	0.974
	10	0.488	0.976
	Mean	0.4863	0.9726
	St. Deviation	0.000823273	0.001646545
67	1	0.488	0.976
	2	0.487	0.974
	3	0.486	0.972
	4	0.485	0.97
	5	0.485	0.97
	6	0.486	0.972
	7	0.486	0.972
	8	0.486	0.972
	9	0.485	0.97
	10	0.486	0.972
	Mean	0.486	0.972
	St. Deviation	0.000942809	0.001885618
73	1	0.486	0.972
	2	0.486	0.972
	3	0.485	0.97
	4	0.485	0.97
	5	0.487	0.974
	6	0.486	0.972
	7	0.486	0.972
	8	0.487	0.974
	9	0.488	0.976
	10	0.485	0.97
	Mean	0.4861	0.9722
	St. Deviation	0.000994429	0.001988858

Appendix B: (Continued)

80	1	0.486	0.972
	2	0.486	0.972
	3	0.486	0.972
	4	0.487	0.974
	5	0.488	0.976
	6	0.486	0.972
	7	0.486	0.972
	8	0.487	0.974
	9	0.486	0.972
	10	0.486	0.972
	Mean	0.4864	0.9728
	St. Deviation	0.000699206	0.001398412
87	1	0.486	0.972
	2	0.486	0.972
	3	0.485	0.97
	4	0.485	0.97
	5	0.487	0.974
	6	0.486	0.972
	7	0.486	0.972
	8	0.487	0.974
	9	0.488	0.976
	10	0.485	0.97
	Mean	0.4861	0.9722
	St. Deviation	0.000994429	0.001988858
94	1	0.486	0.972
	2	0.486	0.972
	3	0.485	0.97
	4	0.487	0.974
	5	0.487	0.974
	6	0.486	0.972
	7	0.486	0.972
	8	0.487	0.974
	9	0.488	0.976
	10	0.488	0.976
	Mean	0.4866	0.9732
	St. Deviation	0.000966092	0.001932184

99	1	0.486	0.972
	2	0.486	0.972
	3	0.486	0.972
	4	0.486	0.972
	5	0.486	0.972
	6	0.487	0.974
	7	0.487	0.974
	8	0.488	0.976
	9	0.488	0.976
	10	0.485	0.97
	Mean	0.4865	0.973
	St. Deviation	0.000971825	0.001943651

Appendix C: 90% and 95% Confidence Interval Values for Ten V$_{max}$ Measurements at Each Temperature and Each Amplifying Circuit.

Table 15. 90% confidence interval values in mV for ten V$_{max}$ measurements at each temperature and each amplifying circuit.

Wien Oscillator	Voltage Mode	Current Mode	Double Current Mode
0.488901139	0.510260516	0.542689431	1.085378863
0.510260516	0.457325062	0.506060784	1.012120949
0.433364405	0.320060915	0.542689431	1.085378863
0.510258656	0.457325062	0.506060784	1.012120949
0.391993087	0.457325062	0.569552588	1.139104555
0.522657036	0.457325062	0.522657036	1.045314072
0.569552588	0.320060915	0.569552588	1.139104555
0.542689431	0.542689431	0.292174477	0.584348335
0.569552588	0.510260516	0.587989011	1.175978641
0.569552588	0.526724751	0.510260516	1.020520411
0.351824171	0.542689431	0.584348335	1.168696669
0.510260516	0.542689431	0.616342154	1.232684308
0.391993087	0.584348335	0.433364405	0.866728811
0.542689431	0.457325062	0.616342154	1.232684308
0.413196895	0.413196895	0.598779022	1.197558045
0.418330037	0.320060915	0.602332307	1.204665234

Appendix C: (Continued)

Table 16. 95% confidence interval values in mV for ten V_{max} measurements at each temperature and each amplifying circuit.

Wien Oscillator	Voltage Mode	Current Mode	Double Current Mode
0.559104328	0.583530779	0.620616287	1.241232575
0.583530779	0.52299412	0.578727993	1.157455277
0.495592862	0.366019689	0.620616287	1.241232575
0.583528653	0.52299412	0.578727993	1.157455277
0.448280877	0.52299412	0.651336827	1.302672946
0.597707364	0.52299412	0.597707364	1.195414728
0.651336827	0.366019689	0.651336827	1.302672946
0.620616287	0.620616287	0.334128931	0.668257152
0.651336827	0.583530779	0.672420607	1.344841923
0.651336827	0.602359177	0.583530779	1.16706085
0.402343953	0.620616287	0.668257152	1.336514305
0.583530779	0.620616287	0.704845087	1.409690174
0.448280877	0.668257152	0.495592862	0.991185724
0.620616287	0.52299412	0.704845087	1.409690174
0.472529421	0.472529421	0.684759998	1.369519996
0.478399651	0.366019689	0.688823513	1.377647734